NASA Technical Memorandum 81839

NASA-TM-81839 19800019876

AN ASSESSMENT OF THE FUTURE ROLES OF THE NATIONAL TRANSONIC FACILITY AND THE LANGLEY TRANSONIC DYNAMICS TUNNEL IN AEROELASTIC AND UNSTEADY AERODYNAMIC TESTING

Perry W. Hanson

June 1980

National Aeronautics and Space Administration

Langley Research Center
Hampton, Virginia 23665

SUMMARY

The technological relationships between the National Transonic Facility (NTF) and the Langley Research Center Transonic Dynamics Tunnel (TDT), including the characteristics and capabilities of the two tunnels, that relate to studies in the fields of aeroelasticity and unsteady aerodynamics are discussed. Scaling considerations for aeroelasticity and unsteady aerodynamics testing in the two facilities are reviewed, and some of the special features (or lack thereof) of the TDT and the NTF that will weigh heavily in any decisions as to the relative merits of conducting a given study in the two tunnels are discussed. For illustrative purposes a fighter and a transport airplane are scaled for tests in the NTF and in the TDT, and the resulting model characteristics are compared. The NTF was designed specifically to meet the need for higher Reynolds number capability for flow simulation in aerodynamic performance testing of aircraft designs. However, it is concluded the NTF can be a valuable tool for evaluating the severity of Reynolds number effects in the areas of dynamic aeroelasticity and unsteady aerodynamics. On the other hand, the TDT was constructed specifically for studies and tests in the field of aeroelasticity. It is concluded that, except for tests requiring the Reynolds number capability of NTF, the TDT will remain the primary facility for tests in the areas of dynamic aeroelasticity and unsteady aerodynamics.

AN ASSESSMENT OF THE FUTURE ROLES OF THE NATIONAL TRANSONIC FACILITY AND THE LANGLEY TRANSONIC DYNAMICS TUNNEL IN AEROELASTIC AND UNSTEADY AERODYNAMIC TESTING

Perry W. Hanson

INTRODUCTION

With the operational availability of the National Transonic Facility (NTF) on the horizon, its capabilities to support research and development studies in the fields of aeroelasticity and unsteady aerodynamics have been compared with those of the Langley Transonic Dynamics Tunnel (TDT) to provide a basis for decisions regarding which tunnel could most advantageously support a particular type of test. This paper discusses the technological relationship between the NTF and the TDT, including the characteristics and capabilities of the two tunnels that relate to tests in these areas.

Fundamentally, the NTF and the TDT were conceived to meet two entirely different needs. In the late sixties, a consensus developed that existing facilities could not meet the ever higher Reynolds number (RN) requirements for flow simulation in aerodynamic performance testing of the newer, large, high performance aircraft designs. The NTF (figure 1) was designed specifically to meet this need for higher RN capability, but it also has some characteristics that make it attractive for aeroelastic testing. On the other hand, the TDT (shown in figure 2) was constructed specifically for studies and tests in the field of aeroelasticity; it has many design features not found in other facilities, including the NTF, that make it uniquely suited for flutter and buffet studies.

This report reviews briefly some factors that are important in aeroelastic and unsteady aerodynamic testing, and some of the special features (or lack thereof) of the TDT and the NTF that are pertinent for studies in these areas. Such features will weigh heavily in any decisions as to the relative merits of conducting a given study in the TDT or the NTF.

SYMBOLS

a	speed of sound, ft/sec (m/sec)
b	characteristic length, ft (m)
C_s/C_{cr}	ratio of structural damping to critical damping
EI	bending stiffness, lb-in^2 (Newton-m^2)
F	Froude number, V^2/bg

f	frequency, Hz
GJ	torsion stiffness, lb-in^2 (Newton-m^2)
g	acceleration due to gravity, 32.2 ft/sec^2 (9.807 m/sec^2)
h	altitude, ft (m)
k	reduced frequency, $b\omega/V$
K_1	P_M/P_A
K_2	T_M/T_A
m	mass per unit length, slugs/ft (kg/m)
M	Mach number, V/a
M_L	local Mach number at which saturation and condensation occur
P	static pressure, lb/sq ft (Newtons/sq m)
P_T	stagnation pressure, lb/sq ft (Newtons/sq m)
q	dynamic pressure, lb/sq ft (kN/sq m)
R	gas constant nominal values: air and nitrogen, 53.3 ft/deg R (29.24 m/deg K); freon, 12.7 ft/deg R (6.97 m/deg K)
RN	Reynolds number, $\rho Vb/\mu$
T	static temperature, deg R (deg K)
T_T	stagnation temperature, deg R (deg K)
V	velocity, ft/sec (m/sec)
v	specific volume per unit weight, cu ft/lb (cu m/kg)
W	weight, lb (kg)
γ	ratio of specific heat nominal values: 1.40 air and nitrogen; 1.14 freon
μ	mass density ratio, $m/\rho b^2$
ρ	fluid free-stream density, slugs/ft^3 (kg/m^3)
σ	fluid free-stream coefficient of viscosity, slugs/ft-sec (kg/m-sec)
ω	circular frequency, $2\pi f$ rad/sec

Subscripts

A airplane

M model

SCALING CONSIDERATIONS FOR AEROELASTIC AND UNSTEADY AERODYNAMICS TESTING

Discussions of the basic requirements for achieving dynamic similarity of model and full-scale aircraft abound in the literature and will only be reviewed here briefly as they apply to transonic aeroelastic and unsteady aerodynamics studies. The similarity requirements are generally deduced by applying the Buckingham II theorem of dimensional analysis or by examining the appropriate governing equations in nondimensional form. For a flexible body completely immersed in a fluid with relative motion between the body and the fluid these procedures result in independent nondimensional parameters which may be thought of as ratios of the potentially significant inertia, viscous, elastic, and gravity forces that act on the body and fluid. The more important ones to be considered are:

$\frac{V}{a}$ Mach number, M (1)

$\frac{b\omega}{V}$ reduced frequency, k (2)

$\frac{m}{\rho b^2}$ mass density ratio, (3)

$\frac{\rho V b}{\sigma}$ Reynolds number, RN (4)

$\frac{V^2}{bg}$ Froude number, F (5)

where

a fluid free-stream speed of sound

V fluid free-stream velocity

ρ fluid free-stream density

σ fluid free-stream coefficient of viscosity

g acceleration due to gravity

b	characteristic length
ω	characteristic oscillation frequency
m	body mass per unit length

These five basic independent dimensionless parameters result from several assumptions regarding characteristics of the body and the fluid. Implicit in the five basic parameters is another, the ratio of the specific heat of the fluid, γ, and, if dissipative forces are considered, a further parameter, the ratio of structural damping to critical damping, C_s/C_{cr}, may be added. From these basic similarity parameters other dependent ratios relating model quantities to full-scale quantities may be derived. If these dimensionless parameters have the same values for the model and the full-scale aircraft and the mass, stiffness, and, to a lesser degree, the damping distributions are the same for the model and full-scale aircraft, then the flexible and rigid body response or behavior of the model will be similar to the aircraft providing the model is geometrically similar to the aircraft, orientation to the airflow is similar to that of the aircraft, and the model is supported in a manner that does not significantly affect the model response or behavior.

The simultaneous satisfaction of all the similarity parameters in a single model or test is not practical. The degree to which the various parameters may be ignored or approximated is a function of the test objective and the available tunnel performance. For example, for static force or pressure measurements on a rigid, stationary model, the reduced frequency, mass density ratio, and Froude number need not be scaled. Although recognized as important, the RN of the model and full-scale airplane could not generally be matched in conventional tunnels because of wind tunnel performance and/or size limitations, and so RN effects have been approximately accounted for by various other means. If one is interested in scaling static deflections of the airplane components (static aeroelastic effects), then the Froude number for the model and airplane must be the same. For measurements of unsteady aerodynamics associated with an oscillating control or buffet pressures on a rigid model, the reduced frequency is important. If the purpose of the test is to predict full-scale buffet loads or flutter characteristics (dynamic aeroelastic tests), then all five basic similarity parameters and the structural damping ratio are important. However, because of conflicting requirements it is not possible to simultaneously satisfy all these similarity parameters. So for high speed dynamic aeroelastic model testing, the recognized importance of reduced frequency, Mach number, and mass density ratio has taken precedence over Reynolds number and Froude number.

These scaling considerations and other facets of aeroelastic and unsteady aerodynamic testing will later be related to the pertinent characteristics and capabilities of the TDT and the NTF.

CHARACTERISTICS OF THE LANGLEY TRANSONIC DYNAMICS TUNNEL

Some characteristics of the TDT are summarized in Figure 3. The most unique feature of the TDT, and that which makes it such a desirable facility for dynamic aeroelastic model tests, is the capability to use Freon-12 gas (dichlorodifluoromethane) as a test medium. The use of this gas for dynamically-scaled aeroelastic model testing has several advantages, the most important of which is its density. For a given tunnel total pressure and temperature, the density of the freon test medium is approximately four times that of air. This is important because, as mentioned previously, a prime requirement for valid interpretation of wind tunnel test results obtained from a dynamically-scaled aeroelastic model relative to the full-scale vehicle is that the ratio of the mass of the model to the mass of a reference volume of the wind tunnel test medium must be the same as the ratio of the mass of the airplane to the mass of the same reference volume of the atmospheric air in which the airplane is operating. That is,

$$\frac{m_M}{\rho_M b_M^2} = \frac{m_A}{\rho_A b_A^2} \quad \text{or} \quad m_M = \frac{\rho_M}{\rho_A}\left(\frac{b_M}{b_A}\right)^2 m_A \quad \text{where} \tag{6}$$

$\frac{b_M}{b_A}$ is the model-airplane geometric scale factor.

Obviously, then, for a given airplane mass and operating altitude (density) and a particular model scale (size), the more dense the tunnel test medium is, the heavier the scaled model can be. Characteristically, it is difficult to fabricate dynamically-scaled aeroelastic models light enough to meet the required scaled weight and strong enough to withstand the loads; hence, the primary attractiveness of the freon gas test medium. Another advantage of the freon test medium is that the speed of sound in freon is about one-half the speed in air at comparable temperatures. Thus, at the same Mach number in air and freon (the model and airplane Mach numbers must be identical for model tests of airplanes which fly fast enough to experience compressibility effects), the velocities in freon are roughly one-half those in air, and because of the lower speed, the scaled model vibration frequencies are half what they would be in air. This reduces the data acquisition frequency requirements, active control oscillation rates, and helicopter model rotor rotation speeds. Also, because of this lower speed of sound (approximately 510 ft/sec at the nominal tunnel operating stagnation temperature of 120° F (322° K), the Froude number and Mach number may be scaled simultaneously by selecting the appropriate model geometric scale factor. (Recall that for compressible flow similarity, $\frac{V_M}{V_A} = \frac{a_M}{a_A}$ (eq. 1) and equation 5, $\frac{b_M}{b_A} = \left(\frac{V_M}{V_A}\right)^2$ (assuming $g_M = g_A$). Therefore $\frac{b_M}{b_A} = \left(\frac{a_M}{a_A}\right)^2$.) The appropriate geometric scale factor to satisfy the Froude number similarity requirements for tests in the TDT varies from about 0.20 to 0.29 depending on the airplane

altitude (speed of sound). For many airplanes or components these are not unrealistically large models for the TDT test section. Further, because of these characteristics of freon, nearly a three-fold increase in RN can be realized for comparable dynamic pressures in air. Also, the use of freon permits the attainment of a given Mach number and dynamic pressure with much less tunnel drive power than would be required in air.

Another prominent feature that contributes to the uniqueness of the TDT facility is its computerized data acquisition system especially designed to process large quantities of dynamic analog data from the models in near real time as needed to guide the conduct of the tests. In addition, the facility has a special capability to rapidly decrease the dynamic pressure, thus increasing the chances of saving expensive models from destruction when flutter is encountered. Special model mounting systems are used to provide near free-flight simulation of the airplane dynamic motions, and special safety screens are provided to prevent tunnel fan damage if a model destructs in the tunnel. The tunnel control room is located immediately adjacent to the test section with large windows providing visual observation of the models--a particularly desirable feature for flutter and buffet testing. Finally, an oscillating vane system in the entrance cone allows sinusoidal variation of the tunnel flow angle for airplane gust response studies. Some of the TDT performance capabilities are shown in Figure 4 (from ref. 1).

For all these special features and unique operational capabilities, the TDT has, as most large tunnels, only a limited RN capability. RN is a parameter which essentially has been neglected in flutter work in the absence of any strong evidence that RN effects are predominantly significant compared to the other recognized important dynamic aeroelastic scaling parameters--mass ratio, Mach number, reduced frequency, and, for static scaled aeroelastic tests, Froude number. The question that needs to be answered is whether RN effects are significant enough for the type of dynamic aeroelastic model tests to warrant the extra expense, model design complications, and other factors associated with testing dynamically-scaled aeroelastic models in the cryogenic environment of the NTF.

CHARACTERISTICS OF THE NATIONAL TRANSONIC FACILITY

Some pertinent characteristics of the NTF, based on information in reference 1, are shown in Figure 5. The primary distinguishing features are the capability to substantially change the stagnation temperature independently of pressure and to operate at very low (cryogenic) temperatures. These features are potentially beneficial for certain kinds of aeroelastic and unsteady aerodynamic testing much like the freon capability of the TDT. For example, the top portion of figure 6 (from p. 16, ref. 2) shows that reducing the stagnation temperature in the NTF from 322° K to the minimum capability of about 80° K (120° F to -316° F) will produce a four-fold increase in density and a decrease in the speed of sound (or velocity, for equivalent Mach numbers) of about 50 percent--about the same effects as testing in freon compared to testing in air. In addition, however, the coefficient of viscosity decreases much more than the change realized between air and freon

so that for comparable dynamic pressures the RN is increased by a factor of six due to the lowered temperature compared to about a factor of three for freon relative to air. However, since models for the TDT can be twice as large as models for the NTF, the net gain in absolute RN is about the same for a given dynamic pressure. But the NTF pressure capability is roughly nine atmospheres at $M = 1.0$ compared to one-half atmosphere for the TDT, thus much higher RN (and correspondingly higher dynamic pressures) are attainable in the NTF as indicated in Figure 7 (values calculated from ref. 3).

In addition to the high RN capability derived from the very low stagnation temperatures and/or high stagnation pressures, the NTF has another characteristic potentially of benefit in dynamic aeroelastic model testing--the ability to adjust fluid temperature independent of density. Recall that for high speed flutter testing the usual requirement is that the model and full-scale values of the three non-dimensional parameters Mach number (V/a), reduced frequency ($b\omega/V$) and mass density ratio ($m/\rho b^2$) must be identical. From these parameters and flexural beam relationships the mass and stiffness properties required for a model to simulate the dynamic aeroelastic behavior of an airplane in level flight at a given speed and altitude are determined; i.e.,

$$M_M = M_A \tag{7}$$

$$(EI)_M = \left(\frac{b_M}{b_A}\right)^4 \frac{q_M}{q_A} (EI)_A \tag{8}$$

$$(GJ)_M = \left(\frac{b_M}{b_A}\right)^4 \frac{q_M}{q_A} (GJ)_A \tag{9}$$

$$m_M = \frac{\rho_M}{\rho_A} \left(\frac{b_M}{b_A}\right)^2 m_A \tag{10}$$

where EI and GJ are the bending and torsional stiffnesses, respectively, q is the dynamic pressure, and the subscripts M and A refer to model and aircraft conditions. By use of the relationship for the speed of sound, $a = (\gamma RT)^{1/2}$, Sutherland's law relating viscosity and temperature, and the equation of state, $Pv = RT$

where P is absolute pressure
v is specific volume per unit weight
T is absolute temperature
R is the gas constant
γ is the ratio of specific heat

the equations which define the various gas flow properties can be expressed in terms of static pressure, static temperature, and Mach number as follows:

$$\rho \alpha \frac{P}{T} \tag{11}$$

$$V \alpha M T^{\frac{1}{2}} \tag{12}$$

$$q \alpha M^2 P \tag{13}$$

$$\sigma \alpha \frac{T^{3/2}}{T+114} \tag{14}$$

$$RN \alpha \left(\frac{T+114}{T^2}\right) PMb \tag{15}$$

Equations (8) - (10) may be written

$$(EI)_M = \left(\frac{b_M}{b_A}\right)^4 \left(\frac{P_M}{P_A}\right) (EI)_A \tag{16}$$

$$(GJ)_M = \left(\frac{b_M}{b_A}\right)^4 \left(\frac{P_M}{P_A}\right) (GJ)_A \tag{17}$$

$$m_M = \left(\frac{b_M}{b_A}\right)^2 \left(\frac{P_M}{P_A}\right)\left(\frac{T_A}{T_M}\right) m_A \tag{18}$$

Once the aircraft stiffness and mass properties $[(EI)_A, (GJ)_A$, and $m_A]$ and flight altitudes (P_A, T_A) and Mach numbers to be simulated have been specified, and a model geometric scale b_M/b_A and a convenient attainable tunnel static pressure and temperature have been chosen, equations (16) - (18) define the model basic physical properties. Note that the required model stiffness is dependent on the ratio of tunnel-to-flight pressures and is independent of the temperatures whereas the required model mass is dependent on both the pressures and temperatures. Lowering T_M alone means the required model will be heavier. Permitting a heavier model for a given stiffness makes model design and construction easier. However, lowering T_M introduces thermal contractions with corresponding stresses and deflections which complicate model design and construction.

The ratio of distributed bending or torsion stiffness to the mass per unit length may be thought of as a "structural efficiency" factor. For an airplane, a high level of stiffness per unit mass is usually desirable.

For a model, however, it is desirable to have a large mass available for a given required stiffness to ease practical model construction. Thus, a small value of EI/m (or GJ/m) would be desirable. For ease of model construction, therefore, the smaller the "structural efficiency" of the model is relative to that of the airplane, the better. Dividing the model/airplane stiffness scale factor (eq. (16)) by the mass scale factor (eq. (18)) gives the model structural efficiency relative to full-scale structural efficiency that results from mass and stiffness scaling, i.e.,

$$\left(\frac{EI}{m}\right)_M = \left(\frac{b_M}{b_A}\right)^2 \left(\frac{T_M}{T_A}\right)\left(\frac{EI}{m}\right)_A \tag{19}$$

Equation (19) presents an anomaly. It shows that not only may the structural efficiency of the model relative to the airplane be decreased by lower model test medium temperatures relative to airplane flight temperature, but that in addition, the model structural efficiency relative to the airplane may be decreased by decreasing the model/airplane geometric scale factor, i.e., by making the model smaller. Practical considerations in model construction, however, dictate increasing difficulty in the fabrication process (closer required tolerances, minimum gage materials, less space available for control actuators, etc.) with decreasing model size. In any assessment of this "structural efficiency" factor ratio of one dynamically scaled model relative to another scaled model the perverse role of the geometric scale factor should not be overlooked.

The model defined by equations (16) through (18) simulates the airplane completely only at the specified flight altitude and at the design tunnel static pressure and temperature. For flight at a different altitude, both the flight density and temperature (speed of sound) will be different. Since the model physical parameters, stiffness, and mass, are fixed (unless a model is made for each flight altitude to be simulated) the tunnel static pressure and temperature would have to be correspondingly changed to maintain precise similarity. It is generally not possible to control the temperature in conventional wind tunnels independently of pressure to simulate the manner in which the temperature and density vary with changes in the full-scale airplane altitude. Therefore, at test conditions away from the model design point, the mass density scaling relationship is not precisely satisfied. This can be compensated for partially by analytically modifying test results for off-design mass ratio effects. Although not usually done, an alternate approach is to construct a series of models, each having the proper stiffness and mass density ratio for each Mach number and altitude to be tested. The use of the NTF could obviate this difficulty since the temperature and density can be independently controlled. However, although it may be desirable to maintain a constant RN throughout the test (due to the sensitivity of model mount interference and model surface smoothness requirements to RN changes) or to separate RN effects on aerodynamic performance from model deformation (dynamic pressure effects, it will be shown in the following discussion that it will

not be possible to maintain a constant RN while matching the changing full-scale mass density ratio.

For mass density similarity between model and airplane,

$$m_M = \left(\frac{b_M}{b_A}\right)^2 \left(\frac{P_M}{P_A}\right)\left(\frac{T_A}{T_M}\right) m_A \quad \text{or} \quad \frac{P_M}{P_A} = \left(\frac{b_A}{b_M}\right)^2 \left(\frac{m_M}{m_A}\right)\left(\frac{T_M}{T_A}\right)$$

and from Mach number and reduced frequency similarity requirements (eqs. (1) and (2)),

$$\frac{T_M}{T_A} = \left(\frac{\omega_M}{\omega_A}\right)^2 \left(\frac{b_M}{b_A}\right)^2$$

The model and airplane reference lengths b, mass m, and frequencies ω are fixed physical characteristics that define the ratios $\frac{P_M}{P_A} = K_1$ and $\frac{T_M}{T_A} = K_2$. The relationships between model and airplane flow characteristics for the same Mach number when model and airplane mass density and reduced frequency similarity requirements are satisfied are then

$$\frac{\rho_M}{\rho_A} = \frac{K_1}{K_2}; \quad \frac{V_M}{V_A} = K_2^{1/2}; \quad \frac{\sigma_M}{\sigma_A} = K_2^{3/2} \left[\frac{T_A + 114}{T_M + 114}\right], \quad T \text{ in deg K and}$$

$$\frac{RN_M}{RN_A} = \frac{K_1}{K_2^{1/2}} \frac{b_M}{b_A} \left[\frac{T_A + 114}{T_M + 114}\right] \tag{20}$$

Thus, the constants that define the relationship between model static pressure and temperature and airplane values for maintaining dynamic similarity also uniquely relate model and airplane density, velocity, and dynamic pressure. However, equation (20) shows that the model/airplane Reynolds number ratio is a function of the absolute values of the model and airplane test media temperatures plus a constant that is common to both. Therefore, the airplane Reynolds number will not be precisely matched by that of the model while mass

density ratio requirements are met. Several examples to follow in the next section will illustrate some of the finer points of dynamic model scaling for the NTF and will show the degree to which full-scale Reynolds number is matched while maintaining dynamic similarity.

The ability to control temperature independently of pressure also allows separation of static aeroelastic (model deformation) effects from RN (scale) effects since the dynamic pressure, and hence aerodynamic forces on the model, can be held constant while the RN can be varied over a relatively wide range as shown in the bottom portion of figure 6 (from page 17, ref. 1). If the static aeroelastic deformations of the model are to be used to predict static aeroelastic deformations of a full-scale airplane, however, the Froude numbers of the model and airplane should be the same. For transonic testing the ratio of the speeds of sound of the airplane and model define the model geometric scale factor necessary for identical model and airplane Froude numbers. For the nominal range of flight temperatures of 59° F to -67° F (288° K to 218° K) and the range of model test temperatures available in the NTF, the required model geometric scale factor ranges from values in excess of 1.0 for an airplane at any realistic temperature and the highest attainable tunnel temperature to a minimum value of 0.34 for the case of an airplane at sea level temperature with the tunnel temperature as low as possible. Except for very small airplane components, 0.34 geometric scale is quite large for the NTF and so some compromise in matching the airplane Froude number will be called for.

Some of the less desirable characteristics of the NTF relative to aeroelastic and unsteady aerodynamic testing are:

(a) Severe temperature environment - The NTF thermal operating envelope may range from about 140° R (78° K) to 635° R (353° K). The resulting thermal stresses and deflections will complicate the design, fabrication, and assessment of natural vibration characteristics of dynamically scaled aeroelastic models. These models are normally fabricated of several materials having different coefficients of expansion. Structural damping may change significantly with large temperature changes so that aeroelastically scaled models may require assessment of natural vibration characteristics at the approximate test temperature. Design and fabrication of close tolerance mechanisms for oscillating models or controls on models for studying unsteady aerodynamics are are also complicated by the thermal environment.

(b) Models can be observed only via TV monitors--a definite disadvantage for flutter and buffet loads tests.

COMPARATIVE MODEL SCALING FOR THE NTF AND THE TDT

Some examples of how the tunnel operating capabilities affect dynamic scaling considerations for flutter testing in the NTF and in the TDT will now be discussed. (The numerical results of these considerations are summarized in figure 11.) First to be considered are a fighter airplane and a transport airplane flutter clearance model for the NTF.

Flutter Clearance Models for the NTF

Fighter airplane model.- Assume that the airplane to be dynamically simulated is a 40,000 lb (18,144 kg) fighter with a 48-foot (14.63 m) wing span and a reference chord b of 15 feet (4.57 m). Assume that the tunnel test is to determine that no flutter occurs in the Mach number range 0.5 to 1.2 at altitudes from 35,000 feet (9144 m) to sea level. The expected critical flutter condition is near $M = 1$ at maximum dynamic pressure (sea level). Therefore, $M = 1$, sea level altitude is the initial airplane flight condition to be simulated. Initial airplane flight conditions are:

$M_A = 1.0$ $\qquad$ $q_a = 1492$ lb/sq ft (71.44 kN/sq m)

$h_A = 0$ ft (m) $\qquad$ $P_A = 2117$ lb/sq ft (101.33 kN/sq m)

$T_A = 519^\circ$ R (288° K) $\qquad$ $\rho_A = 0.002378$ slugs/cu ft (1.226 kg/cu m)

$V_A = 1120$ ft/sec (341 m/sec) $\qquad$ $RN_A = 107 \times 10^6$ (based on b = 15 ft (4.57 m))

Using the criteria that the model wing span in the NTF should not exceed 0.6 of the tunnel width, a 1/10 geometric scale is selected. Presumably the tests are being conducted in the NTF because it is desirable to match or approach full-scale Reynolds numbers. Therefore, the initial tunnel model design condition will be that which produces $RN = 107 \times 10^6$ at $M_M = 1.0$. Referring to figure 8 (the operating boundaries of the NTF at $M = 1.0$ taken from reference 3 and replotted in terms of RN per foot (meter) as a function of stagnation pressure, one sees that the airplane Reynolds number may be matched at stagnation pressures and temperatures as low as 8064 lb/sq ft (386.11 kn/sq m) and 200° R (111.1° K), respectively, and as high as 14,832 psf (710,160 n/m^2) and 300° R (166.7° K), respectively (heavy vertical dashed line). Choosing the lower values as the initial point for model design has the advantage of lower dynamic pressures on the model at the expense of an extremely low temperature environment whereas the higher point subjects the model to almost twice the dynamic pressure but the temperature environment is not quite so severe. First, consider the lower design point:

At $M = 1.0$, $P_{T,M} = 8064$ psf (386,106 n/m^2), and $T_{T,M} = 200^\circ$ R (111.1° K) the model static pressure and temperature are $P_M = 4260.2$ psf (203,980 n/m^2) and $T_M = 166.66^\circ$ R (92.6° K) (static pressures and temperatures derived from reference 4 assuming $\gamma = 1.4$ and $R = 53.3$ ft/deg R ($R = 29.24$ m/deg K)). Thus, $\frac{P_M}{P_A} = 2.013 = K_1$ and $\frac{T_M}{T_A} = 0.321 = K_2$. From equations (16) through (18) the relation between the model and airplane stiffness and mass is

$$(EI)_M = 2.013 \times 10^{-4}(EI)_A \text{ and } m_M = 6.27 \times 10^{-2} m_A$$

$$W_M = 251 \text{ lb } (113.8 \text{ kg})$$

The model vibration frequencies are $\omega_M = 5.67\ \omega_A$. The tunnel stagnation pressures and temperatures necessary to maintain dynamic similarity to the airplane at Mach numbers from 0.5 to 1.2 at three different altitudes are shown in figure 9(a). Also shown is the model dynamic pressure and the lower limits for tunnel stagnation pressure and temperature (from ref. 3). The figure illustrates that both stagnation pressure and temperature have to be varied for each test point where exact dynamic similarity is desired. This may not be a cost effective way to operate the NTF. Also for the model tunnel design point chosen (the lowest stagnation pressure and temperature that will produce full-scale RN) portions of the airplane flight envelope cannot be simulated due to the lower limits on P_T and T_T. The maximum dynamic pressure on the model is about 4300 lb/sq ft (205,885 n/m^2).

An alternative in selecting an initial tunnel design point is to consider the higher pressures and temperature that will produce full-scale RN at $M = 1$ at sea level. For illustrative purposes, choose $P_{T,M} = 14{,}832$ psf (710,160 n/m^2) (near the maximum power limit) and $T_{TM} = 300^\circ$ R (166.7° K) at $M = 1.0$. The static pressure and temperature are 7833 psf (375,046 n/m^2) and 250° R (138.9° K), respectively. Therefore, $\frac{P_M}{P_A} = 3.70 = K_1$;

$\frac{T_M}{T_A} = 0.4817 = K_2$; $(EI)_M = 3.70 \times 10^{-4}(EI)_A$ and $m_M = 7.68 \times 10^{-2}\ m_A$.

and $W_M = 307$ lb (139.3 kg).

The model vibration frequencies are $\omega_M = 6.94\ \omega_A$. Thus, compared to the initial design point chosen previously, a higher model structural efficiency is required and the model vibration frequencies are higher. The model weighs 23 percent more than the previous model. Figure 9(b) depicts the stagnation pressures and temperatures required to maintain model dynamic similarity for various airplane Mach numbers and altitudes. Also shown is the resulting dynamic pressure. For this case, the minimum stagnation temperature limits pose no problem and the minimum stagnation pressure limit at $M = 0.5$ is just adequate to match the airplane mass density ratio at 35,000 ft (10,668 m). However, the upper stagnation pressure limit precludes achieving exact dynamic similarity in the range from $M = 1.07$ at sea level to $M = 1.2$ near 10,000 ft (3048 m). Note also that for this selected initial design point the model would have to withstand dynamic pressures 85 percent greater than the initial design. The lack of capability to simulate the low Mach number, high altitude portion of the Mach number-altitude matrix is not a significant problem since the flutter critical region is usually at the higher Mach number, lower altitudes portion of the flight envelope. Therefore, the first initial design point would be the better choice.

These two examples of dynamic aeroelastic modeling scaling considerations for tests in the NTF illustrate that although in theory the airplane mass density ratio can be matched throughout the airplane flight boundary, in fact even for the NTF the minimum temperature limits and the stagnation pressure range restrict the airplane operating conditions that can be exactly dynamically simulated.

Transport airplane model.- Now consider the dynamic scaling of a large transport aircraft. Assume that the tests are to show freedom from flutter at Mach numbers up to 1.0 at altitudes down to 30,000 feet (9144 m). Assume a wing span of 140 ft (42.67 m), a reference chord of 20 ft (6.10 m) and an empty weight of 135,000 lb (61,235 kg). The geometric scale is chosen to be 0.035 to produce a model span approximately 60 percent of the tunnel width. (b = 0.7 ft (0.21 m).) The initial airplane flight conditions to be simulated are therefore:

$M_A = 1.0$ $\qquad$ $q_A = 442.65$ psf (21,194 n/m^2)

$h_A = 30{,}000$ ft (9144 m) $\qquad$ $P_A = 628.1$ psf (30,074 n/m^2)

$T_A = 412^o$ R (228.9^o K) $\qquad$ $\rho_A = 0.000889$ slugs/ft^3 (0.4582 kg/m^3)

$V_A = 997.92$ fps (304.2 m/sec) $\qquad$ $(RN)_A = 57.2 \times 10^6$

$\sigma_A = 310 \times 10^{-9}$ slug/ft-sec

$(14.843 \times 10^{-6}$ kg/m-sec)

Testing at an initial tunnel model design RN of 81.7×10^6 per foot (268×10^6 per meter) will match the full-scale RN 57.2×10^6, at M = 1.0. From figure 8, this RN may be obtained at stagnation pressures and temperatures ranging from about 15,800 psf (756,508 n/m^2) and 287^o R (159.4^o K), respectively, to approximately 9,911 psf (474,541 n/m^2) and 210^o R (116.7^o K). First, consider the lower pressure and temperature initial design point. For dynamic similarity

$$\frac{P_M}{P_A} = 8.337 = K_1; \quad \frac{T_M}{T_A} = 0.42 = K_2;$$

$$(EI)_M = (0.035)^4 \ (8.337) = 0.1251 \times 10^{-4} (EI)_A \text{ and}$$

$$m_M = \frac{(0.035)^2 \ (8.337)}{0.42} = 0.0243 \ m_A \text{ and}$$

$$W_M = 114.9 \text{ lb } (52.1 \text{ kg})$$

The model vibration frequencies are $\omega_M = 6.48 \ \omega_A$. A comparison of this 0.035-scale transport model with the 0.10-scale fighter model (both having approximately the same wing span--60 percent of tunnel width) shows the transport model must weigh less than one-half the fighter model. Shown in figure 9(c) are the stagnation pressures and temperatures required to maintain exact dynamic similarity at altitudes from sea level to 45,000 ft (13,716 m) at Mach numbers from 0.5 to 1.2. For this model design case altitudes above

30,000 ft (9144 m) cannot be simulated because of the tunnel lower stagnation temperature limits. Conversely altitudes below 3,000 ft (914.4 m) at M = 0.5 and increasing to 10,000 ft (3048 m) at M = 0.8 cannot be simulated because of the maximum stagnation pressure limit. Thus, the airplane altitude-Mach number matrix that can be simulated for the smaller geometric scale transport is much smaller than that for the fighter. If the initial design point for the transport model is taken to be the higher stagnation pressure and temperature that will produce full-scale RN at M = 1.0 in tunnel ($P_{T,M}$ = 15,838 psf (758,328 n/m^2) and $T_{T,M}$ = 287° R (159.4° K)), then $\frac{P_M}{P_A} = 13.32 = K_1$; $\frac{T_M}{T_A} = 0.581 = K_2$; $(EI)_M = (0.035)^4\ (13.32) = 0.1999 \times 10^{-4}\ (EI)_A$ and

$$m_M = \frac{(0.035)^2\ (13.32)}{0.581} + 0.0281\ m_A \text{ and } W_M = 132.7 \text{ lb}$$

(60.2 kg).

It is seen from figure 9(d) that the airplane cannot be exactly dynamically simulated at altitudes below 20,000 ft (6096 m) at Mach numbers above 0.75.

Interestingly, if the model/airplane dynamic similarity requirements are satisfied the Reynolds number of the model and airplane will very nearly be the same--but not exactly. From equation (20)

$$\frac{(RN)_M}{(RM)_A} = \frac{K_1}{K_2^2}\ \frac{b_M}{b_A}\ \left(\frac{K_2 T_A + 114}{T_A + 114}\right)$$

Thus, $(RN)_M/(RN)_A$ is a function of the absolute value of the airplane atmospheric (or model test) temperature. For the scaling examples cited, the ratio of model to airplane Reynolds number varies from 0.966 to 1.090.

If static aeroelastic effects were to be studied, ideally the ratio of model and airplane Froude numbers should be unity. For the examples cited there ratios are:

for the fighter, low pressure and temperature design, $\frac{F_M}{F_A} = 3.21$

for the fighter, high pressure and temperature design, $\frac{F_M}{F_A} = 4.82$

for the transport, low pressure and temperature design, $\frac{F_M}{F_A} = 12.0$

for the transport, high pressure and temperature design, $\frac{F_M}{F_A} = 16.60$

Thus, these models would be inappropriate for static aeroelastic studies that relate model deformations to full-scale values for one-g flight conditions.

Flutter Clearance Models for the Transonic Dynamics Tunnel (TDT)

Now consider the scaling of these same flight conditions (fighter at sea level, $M = 1.0$ and transport at 30,000 ft (9144 m), $M = 1.0$) for tests in the TDT. Using the same maximum model span criteria used for the NTF (span less than approximately 60 percent of tunnel width) leads to a model geometric scale of 0.2 for the fighter and 0.07 for the transport. The model span and reference chord for the fighter will be 9.6 feet (2.93 m) and 3.0 feet (0.91 m), respectively, and for the transport, 9.8 feet (2.99 m) and 1.4 feet (0.43 m), respectively.

Fighter airplane model.- Testing at full-scale Reynolds number in the TDT is not possible so the rationale in selecting the tunnel model design point is to select as high a density as possible at the expected critical Mach number (in this case $M = 1.0$) that will produce a model-to-airplane dynamic pressure ratio such that the scaled airplane dynamic pressure at the maximum Mach number of the flight boundary to be cleared can be attained in the tunnel. The maximum attainable dynamic pressure in the TDT at $M = 1.2$ in Freon is approximately 240 lb/sq ft (13.41 kN/sq m) (ref. 2). If the fighter flight flutter boundary to be cleared extends to $M = 1.2$ at sea level, the maximum dynamic pressure ratio q_M/q_A that can be utilized is 0.13. Therefore, the model will be designed to simulate the airplane sea level flight condition at $M = 1$ and $q_M = 194$ lb/sq ft (9.29 kN/sq m) in the TDT. From equation (8) the model/airplane stiffness scale factor is

$$\frac{(EI)_M}{(EI)_A} = (0.2)^4 \ (0.13) = 2.08 \times 10^{-4}$$

Assuming a nominal tunnel operating stagnation temperature $T_{M,T}$ of 115° F or 575° R (319.4° K) which produces a static temperature of 78° F or 538° R (298.9° K) the density ratio at this model design point is

$$\frac{\rho_M}{\rho_A} = \frac{1.4981 \times 10^{-3}}{2.378 \times 10^{-3}} = 0.630 \text{ and } P_{M,T} = 593.3 \text{ lb/sq ft } (28.41 \text{ kN/sq m})$$

$$P_M = 342.3 \text{ lb/sq ft } (16.39 \text{ kN/sq m})$$

$$\frac{P_M}{P_A} = 0.162$$

The model/airplane mass scale factor (from eq. (3)) is

$$\frac{m_M}{m_A} = (0.2)^2 \ (0.630) = 2.52 \times 10^{-2}$$

The model weight is 202 lbs (91.6 kg) and the model vibration frequencies are (from eq. (2)) $\omega_m = 2.27 \ \omega_A$.

A comparison of this TDT fighter model with the NTF fighter models (high pressure/temperature and low pressure/temperature designs) shows that the TDT model is twice as large but weighs less than either of the NTF models. The TDT model vibration frequencies are less than half those of the NTF models.

For this model true dynamic similarity can be achieved only at the model design point ($M_M = 1.0$, $q_M = 194$ psf (9289 n/m^2). Since the tunnel temperature cannot be maintained as a controlled variable the ratio of model/airplane temperature and density will vary as Mach number and pressure are changed. The variation of some of the scaling parameters is shown in figure 10(a). The ratio of model mass density to airplane mass density will differ from the desired value of unity, varying from 0.977 at $M = 1.2$ at sea level to 1.321 at $M = 0.5$ at a simulated 30,000 feet (9144 m) altitude. Similarly, the reduced frequency ratio varies from 1.01 to 0.87. Also, the model Reynolds number will vary from only 8.1 percent of full scale at $M = 1.2$ at sea level to only 5.5 percent of full scale at $M = 0.5$, 30,000 ft (9144 m) altitude. The ratio of model Froude number to airplane Froude number is very nearly unity (varying from 1.01 for the simulated sea level $M = 1.2$ condition to 1.36 at $M = 0.5$ at 30,000 ft (9144 m)). Thus, model static deformations will very nearly approximate those of the full-scale airplane in one-g flight. The maximum dynamic pressure on the TDT model is 280 psf (13,407 n/m^2) compared to 4300 psf for the NTF low pressure model and 6200 psf (maximum attainable) for the NTF high pressure model.

Transport airplane model.- As was the case for the NTF, the maximum flight conditions for the transport airplane are chosen to be Mach numbers up to 1.0 at altitudes down to 30,000 ft (9144 m). The maximum airplane dynamic pressure (at $M = 1.0$) is therefore 443 psf (21,211 n/m^2). A tunnel model design point is chosen at a model dynamic pressure of 300 psf (14,364 n/m^2), slightly

below the normal maximum tunnel capability at M = 1.0. Therefore, the dynamic pressure ratio q_M/q_A is 0.677.

The model/airplane stiffness scale factor is

$$\frac{(EI)_M}{(EI)_A} = (0.07)^4 \ (0.677) = 0.1626 \times 10^{-4}$$

From reference 2, $P_{M,T}$ = 917.4 psf (43,925 n/m^2); P_M = 529.3 psf (25,343 n/m^2) and $\frac{P_M}{P_A}$ = 0.843.

Again assuming a nominal tunnel stagnation temperature of 115° F or 575° R (319.4° K) the model velocity is (ref. 2) 507 fps and the tunnel density is 0.0023342 slugs/ft^3 (1.203 kg/m^3).

The density ratio,

$$\frac{\rho_M}{\rho_A} = 2.626$$

and the model/airplane mass scale factor is

$$\frac{m_M}{m_A} = (0.07)^2 \ (2.626) = 1.287 \times 10^{-2}$$

The model weight is 121.6 lbs (55.2 kg) and the model vibration frequencies are $\omega_M = 7.26 \ \omega_A$.

A comparison of this TDT transport model with the NTF transport models (high pressure/temperature and low pressure/temperature designs) shows the mass and the vibration frequencies are about the same as the NTF low pressure/temperature model although the TDT model is twice the size of the NTF model. The dynamic pressure at M = 1.0, 30,000 ft (9140 m) simulated altitude for the TDT transport model is 300 psf (14,364 n/m^2) compared to 3690 psf (176,678 n/m^2) for the NTF low pressure model and 5,897 psf (282,350 n/m^2) for the NTF high pressure model.

The deviations of the mass density and reduced frequency scaling parameters from the desired value of unity due to the lack of capability to maintain a constant T_M/T_A in the TDT are shown in figure 10(b) along with the model/airplane Reynolds number ratio for the tunnel design point chosen for the transport model (M = 1.0, 30,000 ft (9144 m)). Simulated airplane altitudes below 10,000 ft (3048 m) cannot be attained at Mach numbers greater than 0.7 in the TDT. (In the example, flutter clearance only needed to be demonstrated at

altitudes down to 30,000 ft (9144 m). Within the dynamic pressure capabilities of the TDT the reduced frequency scaling parameter is within 6 percent of unity and the mass density ratio is within 11 percent (M = 0.7, 10,000 ft (3048 m)). The model Reynolds number is 10 to 12 percent of full scale and the ratio of Froude numbers varies from 6.5 to 7.5.

In summary, based on the examples cited above and summarized in figure 11, it appears that dynamically-scaled aeroelastic models for the NTF have the following characteristics relative to those for the TDT:

NTF models are about one-half the geometric size of TDT models, weigh about the same or slightly more and have natural vibration frequencies two and one-half to three times those of TDT models. In the NTF the mass density and reduced frequency scaling parameters can be satisfied throughout most of the airplane operating envelope whereas in the TDT away from the design point they varied from the desired values by up to approximately 30 percent. Full-scale RN over most of the airplane operating envelopes could be achieved in the NTF. RN in the TDT were generally an order of magnitude lower than full scale. NTF models were subjected to dynamic pressures roughly 20 times those on the TDT models. Test static temperatures in the NTF varied from -334° F or 126° R (70.0° K) to -160° F or 300° R (166.7°) compared to 105° F to 64° F or 565° R (313.9° K) to 524° R (291.1° K) in the TDT.

In addition to comparisons of physical characteristics of flutter models scaled for the NTF and for the TDT, comparisons of direct tunnel operating costs for flutter testing is of interest. Unlike static force or pressure test procedures which entail operating the tunnel in a manner such that a particular test point (Mach number pressure, and angle of attack - and temperature in the NTF) is achieved as rapidly as possible, flutter test procedures call for cautious changes in tunnel parameters to minimize the risk of destroying the model while probing for the flutter boundary. This is an expensive operational procedure in the NTF. To illustrate, suppose it is desired to establish the transonic flutter boundary of the transport plane (low pressure and temperature design) that was used in the model scaling discussions. Figure 12 depicts schematically a "typical" flutter boundary, the airplane operating boundary (which includes a 20 percent of design velocity flutter safety margin) and a minimum process for establishing the flutter boundary. To establish a basis for estimating the tunnel direct operating costs for a minimal definition of the transonic flutter boundary in the NTF and in the TDT, it is assumed that five Mach number "runs" or "sweeps" are required as shown in the figure. Since the transonic "dip" in the flutter boundary is not really known until established by the test, the first several sweeps are exploratory. The procedure is to increase Mach number and dynamic pressure until the maximum Mach number is reached or until flutter is encountered. The Mach number (and dynamic pressure) is then reduced to a level below that where the minimum part of the flutter boundary is expected to occur (say to M = 0.8). The tunnel pressure then is increased (simulating a lower airplane altitude) and another Mach sweep is made. The unknown flutter boundary must be approached slowly to minimize risk to the model. In practice, such Mach sweeps in the TDT take 10 to 15 minutes. For purposes of comparing the cost of such a test in

the NTF and in the TDT it is assumed that the five sweeps start and end at the same Mach number in the two tunnels and have the same durations. The costs considered are the electrical power and the cost of Freon and nitrogen consumed in establishing the proper pressure levels and in making the Mach number sweeps. The electrical power rate is assumed to be $0.05 per kwh. The cost of Freon and nitrogen is assumed to be $872 and $70 per ton, respectively. Based on these assumptions, the cost of determining the flutter boundary as shown in the illustrative example is:

	NTF	TDT
Electrical power	2,320	1,050
Gas	69,000	990
TOTAL	$71,320	$2,240

The Reynolds number range for the NTF tests, however, is 86 to 150 million (very nearly full scale) compared to 4.2 to 8.2 million for the TDT tests. Also, for the NTF tests the mass density and reduced frequency scaling parameters would have been satisfied completely whereas in the TDT tests actual values would have varied from the desired values by about 10 percent except at the model design point.

With this background of dynamic model scaling considerations and comparative operating characteristics and features of the TDT relative to the NTF, it may be instructive to review the technology areas supported by the TDT in the past, and presently scheduled for the next 3 years, to help assess the future roles of the NTF and the TDT in aeroelastic and unsteady aerodynamic testing.

EVALUATION OF NTF TESTING CAPABILITIES IN TECHNOLOGY AREAS SUPPORTED BY THE TDT

Whereas most wind tunnels are used almost exclusively for aerodynamic performance type testing--i.e., precise measurements of overall steady aerodynamic forces acting on the model (drag, lift, moments, etc.) or pressure distributions over the model--the TDT has been used for a variety of dynamic tests. Figure 13 depicts the TDT and some of the important research and development areas it supports. The TDT has been used to verify the flutter and aeroelastic characteristics of most U.S. high-performance aircraft designs; for studies of the aeroelastic characteristics of wings employing new aerodynamic concepts; for rotorcraft and active controls aeroelastic research; for flutter, buffet, and ground wind loads testing of space launch vehicles; and for basic research into unsteady aerodynamic flow caused by dynamic motions of lifting surfaces.

Historically, about 40 percent of the scheduled tests have been devoted to development studies of aeroelastic problems of specific vehicles in support of national programs. The majority of these tests are concerned with the

prediction of full-scale flutter and buffet characteristics using dynamically-scaled cable-mounted models. The major tests are shown in figure 14. Many of these tests disclosed design problems and provided information for successful flutter "fixes" (refs. 5 to 7, for example). As discussed in the section on comparative model scaling for the NTF and the TDT, dynamically-scaled aeroelastic models tested in conventional tunnels represent the full-scale airplane precisely only at the tunnel "design point." Over the range of Mach numbers and altitudes of interest in these tests the mass density and reduced frequency ratios deviated from the desired value of unity by a maximum of about 10 percent. In the NTF, the scaling could have been exact. However, the feasibility of testing cable-mounted models in the NTF has not been established. Experience has shown that for many aircraft configurations the simulation of the fuselage bending modes and the minimum restraint on "rigid body" degrees of freedom provided by cable-mounted models are necessary for adequate dynamic aeroelastic scaling. Cable tension-to-weight ratio requirements (for stability) and drag loads dictate the use of 1/8-inch steel cables in the TDT. With dynamic pressures from three to 30 times higher in the NTF, significantly large cables may be required. Because of the added complications and expense of designing, building, and testing these very sophisticated dynamic models for the cryogenic environment of the NTF, it is unlikely that tests of this nature will routinely be conducted in the NTF until it is established that Reynolds number effects are significant in the classical flutter phenomenon.

The TDT has been utilized also to determine the ground wind load characteristics of most U. S. space launch vehicles while erected on the pad prior to launch (ref. 8, for example). These wind loads and the dynamic responses to them cannot be predicted by theory but are frequently the design loads for the vehicle first stages. Some of the major ground wind load studies conducted in the TDT are shown in figure 15. The relatively large scale models permitted by the TDT 16-foot test section (desirable for simulation of launch vehicle detail and the associated launch pad gantry and other nearby structures) and the wind azimuth variation capability provided by the floor-mounted turntable are very desirable tunnel characteristics for this type test. The higher Reynolds number capability of the NTF may outweigh the size advantage of the TDT but the NTF does not have a floor-mounted turntable.

In addition to supporting these technological areas, the unique capabilities of the TDT have been used for buffet response tests on several launch vehicles and aircraft (refs. 9 to 11, for example), for determining the dynamic deployment characteristics of the Viking Lander deceleration system, reference 12, and for simulation of the Martian atmosphere for Viking Lander meteorological instrumentation (ref. 13). The TDT also has played a significant role in the determination of the aeroelastic characteristics of new helicopter rotor blade concepts such as the teetering rotor, the hingeless rotor, and the flex-hinge rotor (refs. 14 to 16, for example). About one-fourth of the TDT yearly test schedule is devoted to rotorcraft dynamics utilizing a specially built rotor test rig that allows vibration inputs to the rotating blades under a range of speeds from hover to transonic tip speeds. Most of these studies required specialized tunnel capabilities. For example, parachute deployment studies of shock loads and stability require a long test

section viewing area due to the usual relatively great distance between the canopy and its attachment to the forebody. Also, the ability to decrease rapidly the tunnel dynamic pressure on deployment of the parachute is desirable to simulate the slowing of the forebody as the parachute drag becomes effective. For buffet loads studies under high lift conditions, direct viewing of the model is highly desirable to permit detection of incipient model failure. Also, direct viewing is necessary for helicopter rotor tests to permit blade balancing and tracking. The helicopter rotor studies require a rotor mount system capable of rotating the blades at the desired RPM, changing the blade collective and cyclic pitch angles, the rotor plane angle, vibration input capability, and a means of measuring the loads and vibration characteristics of the rotating blades. Whether these types of tests are appropriate for the NTF will have to be determined by weighing the need for high Reynolds number testing against the compromises necessary in desirable specialized tunnel features for the individual tests that are not available in the NTF.

A factor to be considered in assessing whether a particular test is suitable for the NTF is the degree of risk of model destruction. Testing dynamically-scaled aeroelastic models for flutter and buffet loads necessarily involves considerably more chance of the model "going down the tunnel" than tests of force and pressure models. Although tunnel facility managers generally require load safety factors of three or greater for models to be tested, scaled flutter models frequently have ctitical load safety factors not much greater than one. Strength is built into the model only to the extent that it does not significantly compromise the required scaled stiffness. Consequently, flutter models are much more likely to fail than aerodynamic performance models. The risk of model destruction is accepted in TDT flutter tests because the fan blades are well protected by special screening to catch model debris.

The assessment of the future role of the NTF in aeroelastic (dynamic) and unsteady aerodynamic testing is complicated by the uncertainty of the difficulty of fabricating suitable models and oscillation mechanisms for the NTF cryogenic environment. The degree of this difficulty needs to be established and weighed against the obvious advantages offered by the NTF--high Reynolds numbers, the capability to operate in a manner to maintain precise dynamic model similarity for various flight conditions rather than only at the tunnel model "design point," and the capability to vary Reynolds number and dynamic pressure independently. Further, the significance of Reynolds number effects on flutter, buffet on-set and loads, and on unsteady aerodynamics needs to be established.

PLAN FOR UTILIZING UNIQUE CAPABILITIES OF THE NTF FOR STUDIES IN AEROELASTICITY AND UNSTEADY AERODYNAMICS

Some of the first studies in the NTF should be designed to:

1. Establish significance of Reynolds number effects on flutter and buffet characteristics of several representative wings as a function of angle of attack and Mach number by use of relatively simple models.

2. Evaluate effects of Reynolds number on unsteady pressures on oscillating wings and controls as a function of frequency, amplitude, and Mach number.

3. Establish the feasibility of conducting flutter clearance tests in the NTF using dynamically-scaled aeroelastic models by actually fabricating and testing such a model.

In the following sections, a rudimentary plan is suggested for an initial step in each of these efforts.

Reynolds number effects on flutter and buffet.- At transonic speeds the flutter boundary of an airplane or model can be defined in terms of the dynamic pressure at which flutter occurs for a given Mach number. With the capability of the NTF to vary dynamic pressure at a given Mach number while holding RN constant, a Mach number-dynamic pressure flutter boundary can be established for a simple flutter model (say rectangular, solid metal, sidewall-mounted wing with AR $\approx$ 4) for a nominally low, intermediate, and high Reynolds number. A problem arises however, in that as Reynolds number is changed, μ, the mass-density ratio flutter parameter changes also. (From eqs. (3) and (11), $\mu \approx \frac{m}{\rho} \approx m\frac{T}{P}$. As Reynolds number changes, static pressure and temperature change according to equation (15) rather than the simple ratio T/P.) For example, if the model mentioned above had a 65A009 solid magnesium airfoil with a 10-inch (0.25 m) chord, the estimated flutter conditions at M = 1.0 and a RN = 20×10^6 produce a mass density ratio that is two and one-half times the mass-density ratio at M = 1.0 and RN = 90×10^6. However, a fortunate characteristic of magnesium, aluminum, and steel provides a solution to this dilemma. The ratio of the moduli of torsional and bending elasticity to the material density is essentially constant so that geometrically similar solid models made of these materials will have the same natural frequencies and therefore will flutter at the same mass density ratio for a given Mach number. The densities of aluminum and steel are respectively approximately 1.56 and 4.48 times that of magnesium. Therefore, if the magnesium wing is tested at a RN = 20×10^6, the aluminum wing at RN = 31×10^6, and the steel wing of RN = 89×10^6 the mass density ratio at the flutter dynamic pressure and Mach number will be the same for all three Reynolds numbers (except for possible

Reynolds number effects.) This is shown in figure 16 which shows the flutter boundaries of the three wings as a function of mass density ratio and stagnation pressure and in figure 17 which tabulates the estimated tunnel conditions and mass density ratios for the three test Reynolds number. The flutter dynamic pressures were estimated using preliminary design empirical methods. Possible effects of cryogenic temperatures on the stiffness and damping characteristics of the models have not been considered. To minimize loads problems the models should be tested at zero lift conditions. In conducting the tests, as P_T is increased at constant M to increase q until flutter is reached the T_T is adjusted to maintain the RN constant.

These same models may be used to evaluate Reynolds number effects on buffet loads by measuring model response and damping at constant values of the mass-density ratio parameter at the same Reynolds numbers used for the flutter study, but at dynamic pressures at each Mach number that are below those that would produce flutter or overload the model for the maximum angle of attack to be used. The procedure would entail setting the tunnel to the desired RN, M, and q and measuring the model response and damping as angle of attack is changed from low to high values.

This kind of study should be among the first studies to be scheduled in the NTF since the results will bear directly on the question of the necessity or desirability of conducting more sophisticated "flutter clearance" and buffet loads tests in the NTF.

Reynolds number effects on unsteady aerodynamics.- A wing or control surface that is oscillating superimposes on the normal static pressure distribution unsteady components which influence the flutter and buffet characteristics of the wing and the loads and hinge moments of rapidly moving controls used for flutter suppression and gust load alleviation. The degree to which Reynolds number affects these unsteady pressures needs to be defined. An initial study could utilize a "rigid" lifting surface which is forced to pitch harmonically about a spanwise axis over a range of reduced frequencies, static angles of attack, and Reynolds numbers. To minimize unknown model static deformation effects, the measurements should be made with the dynamic pressure held essentially constant and at as low a value as possible that permits a significantly large range of Reynolds numbers. This study necessarily involves the design of a sidewall mount for the NTF that includes an oscillating mechanism and a remotely-controllable static angle-of-attack capability. Such a sidewall mount is currently being planned which will be compatible with an oscillating pressure model being built under Air Force contract for testing in the NRL tunnel in the Netherlands. This model, which also is being designed to withstand the loads and cryogenic environment of the NTF, is expected to be available for testing in the NTF in 1983. The all-steel model will have a wing semispan of about one meter (3.28 ft), a root chord of approximately one meter (3.28 ft) and a mean aerodynamic chord of approximately 3/4 m (2.46 ft).

Dynamically-scaled aeroelastic "pathfinder" model.- If it is shown that Reynolds number effects on flutter are significant, then, until a data base of these effects are established sufficient to allow extrapolation of lower

Reynolds number data to full scale, the RN capabilities of the NTF may be desirable for "flutter clearance" tests. Such tests utilize sophisticated dynamically-scaled aeroelastic models to show that flutter will not occur in the required flutter safety margin of the airplane operating envelope. In order to match the stiffness and mass distributions of the full-scale airplane many different materials have necessarily been used in the fabrication of this type model. These include aluminum, steel, lead, wood, fiberglass and other composite materials, and different bonding agents. Potential problems associated with subjecting such a model to a cryogenic environment include the effects of changes in structural damping, misalignment and distortions due to different coefficients of expansion of the various materials, embrittlement, and changes in stiffness properties. The degree to which such materials will have to be used in flutter clearance models designed for the NTF needs to be established. For example, the weight of the complete transport model discussed in the section on comparative model scaling for the NTF and the TDT varied from 115 lb (52.2 kg) to 133 lb (60.3 kg) depending on the tunnel temperature and pressure design points. If this model has approximately the geometry of the B-720 transport and were made of solid aluminum it would weigh approximately 125 lb (56.7 kg). In a gross sense, it would appear that the use of several different materials might not be necessary for this model. However, one would have to look at the airplane mass and stiffness distributions in detail to determine whether simulation could be achieved by judicious machining of metal. A good way to assess the potential problems would be to actually design and build a dynamically-scaled aeroelastic model of an actual airplane design. A reasonable approach would be to first consider a sidewall-mounted semispan wing model only and then proceed to the more difficult sting-mounted complete model. If these prove technically and economically feasible, then consideration could be given to a study of the feasibility of cable-mounted models.

CONCLUDING REMARKS

Scaling considerations for aeroelastic and unsteady aerodynamics testing have been reviewed relative to model testing in the NTF and the TDT. The unique capabilities of the two tunnels have been reviewed. Certain capabilities of the NTF are found to be attractive for flutter testing such as the ability to match properly in a single model the mass ratio and Mach number scaling parameters for most usual full-scale aircraft variations in altitude and speed, and the capability to achieve a low speed of sound (by use of very low temperatures) which permits heavier dynamically-scaled aeroelastic models for a given stiffness much the same as is achieved in the TDT by the use of a dense Freon test medium. The realization of this advantage depends on overcoming the practical difficulties of constructing such models for the NTF cryogenic environment.

The capability of the NTF to change Reynolds number while holding dynamic pressure constant, and vice versa, allows separation of Reynolds number effects from model static deformation effects (proportional to dynamic pressure). This has limited usefulness for determining Reynolds number effects on flutter

since the important flutter parameter, mass density ratio changes with Reynolds number.

Since Reynolds number effects are likely to be more pronounced in situations where the boundary layer characteristics are important such as tests for unsteady aerodynamic force, moment, and pressure measurements due to lifting surface and control surface motions, the high Reynolds number capability could be especially useful for those studies where the data will be related to full-scale conditions.

The NTF offers a maximum Reynolds number capability 8 and 16 times that of the TDT at M=0.7 and at M=1.0 respectively although at the expense of dynamic pressures about 13 and 22 times respectively those in the TDT. The NTF can be a valuable tool for evaluating the severity of Reynolds number effects in the areas of dynamic aeroelasticity and unsteady aerodynamics. A firmer basis for judging whether particular studies in these areas should be conducted in the NTF can be provided by the prevously discussed evaluation studies. The TDT, because of its special capabilities, equipment, and lower operating cost, is expected to remain the primary facility for testing in the areas of dynamic aeroelasticity and unsteady aerodynamics.

REFERENCES

1. Staff of Aeroelasticity Branch: The Langley Transonic Dynamics Tunnel. LWP-799. Sept. 1969.

2. Baals, Donald D. (Editor): High Reynolds Research. NASA CP-2009. Proceedings of Workshop, LRC, Hampton, VA, Oct. 27-28, 1976.

3. Gloss, Blair B.: National Transonic Facility Calculated Performance Maps. RN 20-10A, May 2, 1977.

4. Ames Research Staff: Equations, Tables, and Charts for Compressible Flow. NACA TR 1135, 1953.

5. Reed, Wilmer H., III: Review of Propeller-Rotor Whirl Flutter. NASA TR R-264, July 1967.

6. Sandford, Maynard C.; Ruhlin, Charles L.; and Yates, E. Carson, Jr.: Subsonic and Transonic Flutter and Flow Investigations of the T-Tail of a Large Multijet Cargo Airplane. NASA TN D-4316, Feb. 1968.

7. Foughner, J. T., Jr.; and Bensinger, C. T.: F-16 Flutter Model Studies with External Wing Stores. NASA TM 74078. Nov. 1977.

8. Farmer, Moses G.; and Jones, George W., Jr.: Summary of Langley Wind Tunnel Studies of Ground-Wind Loads on Launch Vehicles. Compilation of Papers Presented at NASA LRC Meeting of Ground Wind Load Problems in Relation to Launch Vehicles, June 7-8, 1966. TM X-57779.

9. Hanson, Perry W.: Evaluation of an Aeroelastic Model Technique for Predicting Airplane Buffet Loads. NASA TN D-7066, Feb. 1973.

10. Doggett, Robert V., Jr.; and Hanson, Perry W.: Wind Tunnel Buffet Pressure Investigation on the Lower Nose Portion of the RF-4C Aircraft. LWP-222, June 1966.

11. Hanson, Perry W.; and Doggett, R. V.: Aerodynamic Damping and Buffet Response of an Aeroelastic Model of the Saturn I Block II Launch Vehicle. NASA TN D-2713, March 1965.

12. Foughner, Jerome T., Jr.; and Alexander, William C.: Transonic Wind Tunnel Studies of Cross, Disk-Gap-Band, and Hemisflo Parachutes. NASA TN D-7759, Nov. 1974.

13. Green, George C.; Keafer, Lloyd S., Jr.; Marple, C. G.; and Foughner, Jerome T., Jr.: Flow-Field Measurements Around a Mars Lander Model Using Hot-Film Anemometers Under Simulated Mars Surface Conditions. TN D-6820, Sept. 1972.

14. White, Bill; and Weller, William: The Flexhinge Rotor. Presented at the AHS Mideast Region Symposium on Rotor Technology, Essington, PA. August 1976.

15. Hammond, C. E.; and Weller, W. H.: Recent Experiences in the Testing of a Generalized Rotor Aeroelastic Model at Langley Research Center. Second European Rotorcraft and Powered Lift Aircraft Forum, Sept. 21-22, 1976.

16. Weller, William H.: Load and Stability Measurements on a Soft-Inplane Rotor System Incorporating Elastomeric Lead-Lag Dampers. NASA TN D-8437, July 1977.

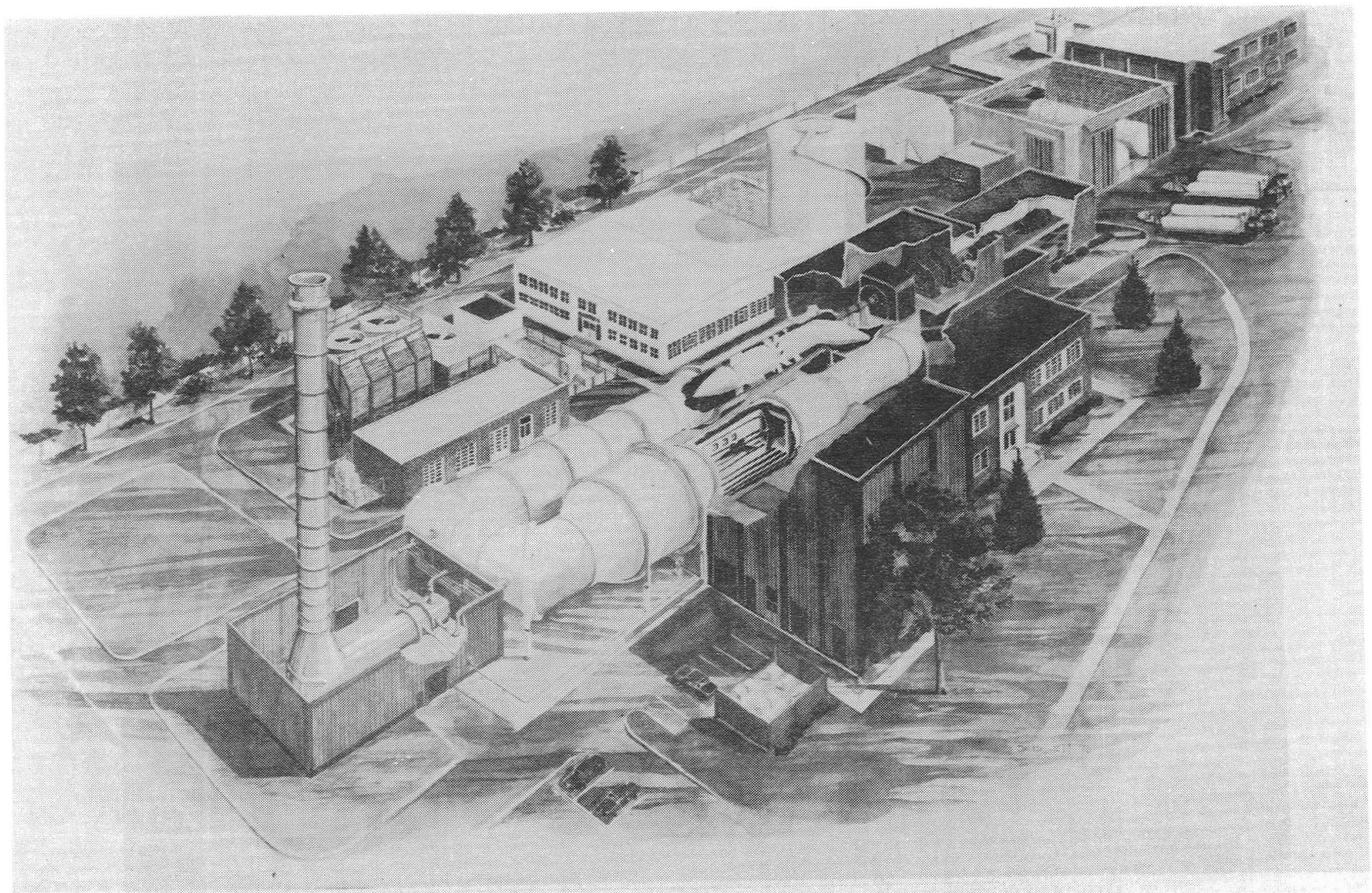

Figure 1.- National Transonic Facility

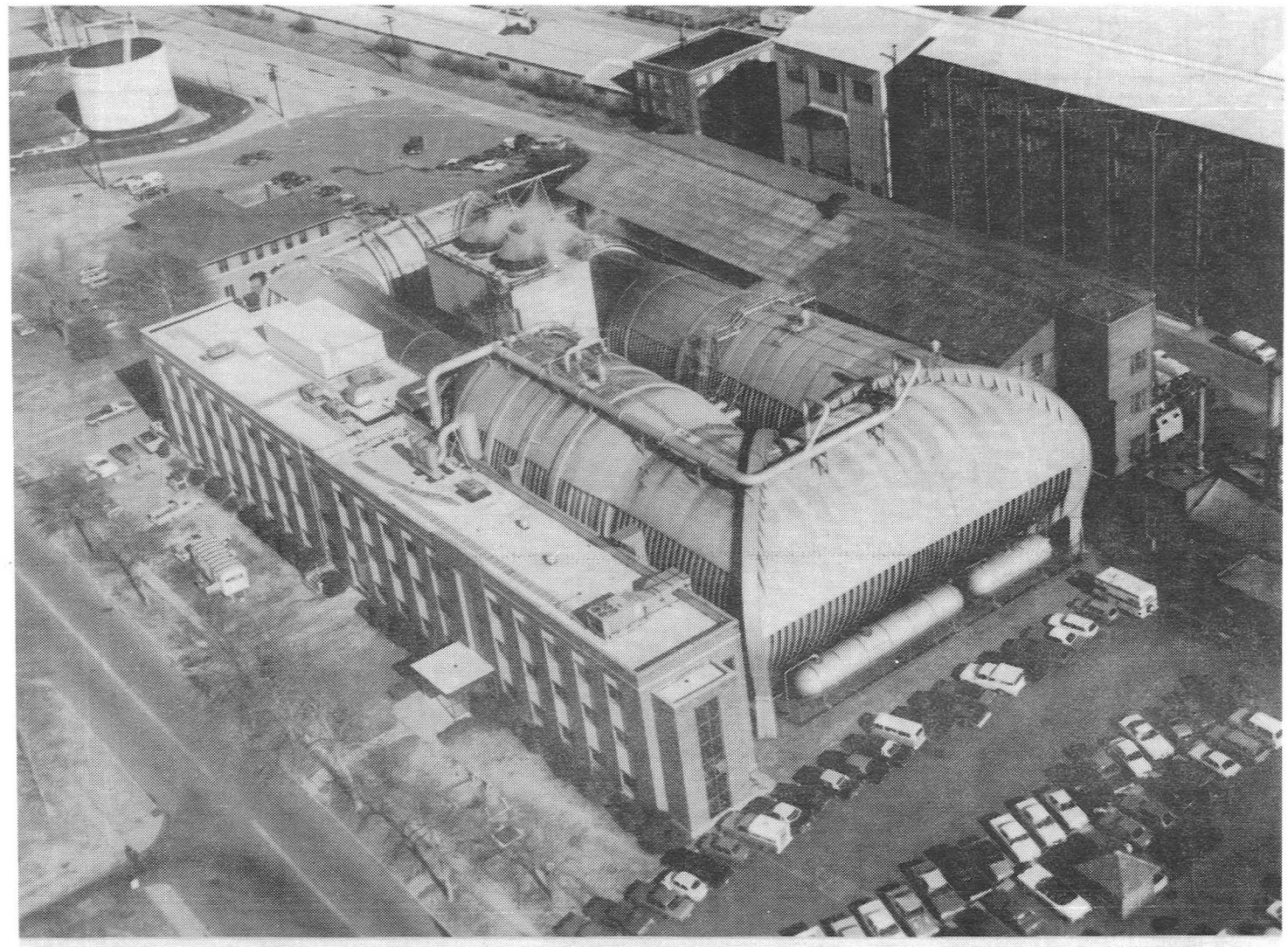

Figure 2.- Langley Research Center Transonic Dynamics Tunnel.

- TRANSONIC MACH NUMBER CAPABILITY - NEAR ZERO TO 1.2
- TEST SECTION SIZE - 16-FT BY 16-FT (4.88m BY 4.88m)
- FREON-12 TEST MEDIUM
  - ALLOWS CONSTRUCTION OF HEAVIER DYNAMICALLY SCALED AEROELASTIC MODELS, REDUCING COST AND FACILITATES INCORPORATION OF ACTIVE CONTROLS
  - REDUCES DATA ACQUISITION FREQUENCY REQUIREMENTS, ACTIVE CONTROL OSCILLATION RATES AND HELICOPTER BLADE ROTATION SPEEDS
  - THREEFOLD INCREASE IN RN FOR COMPARABLE Q IN AIR
  - LOW TUNNEL DRIVE POWER REQUIRED - 20,000HP DRIVE MOTOR
- SPECIAL COMPUTERIZED DATA ACQUISITION SYSTEM DESIGNED FOR DYNAMIC DATA PROCESSING IN ALMOST REAL TIME
- CAPABILITY TO RAPIDLY DECREASE M AND Q
- SPECIAL MODEL MOUNT SYSTEMS PROVIDE NEAR FREE FLIGHT SIMULATION OF AIRPLANE DYNAMIC MOTIONS
- SPECIAL SAFETY SCREENS PROTECT FAN FROM MODEL DEBRIS
- EXCELLENT VISIBILITY OF MODEL
- OSCILLATING FLOW FIELD CAPABILITY FOR GUST RESPONSE STUDIES

Figure 3.- Characteristics of the Langley Transonic Dynamics Tunnel

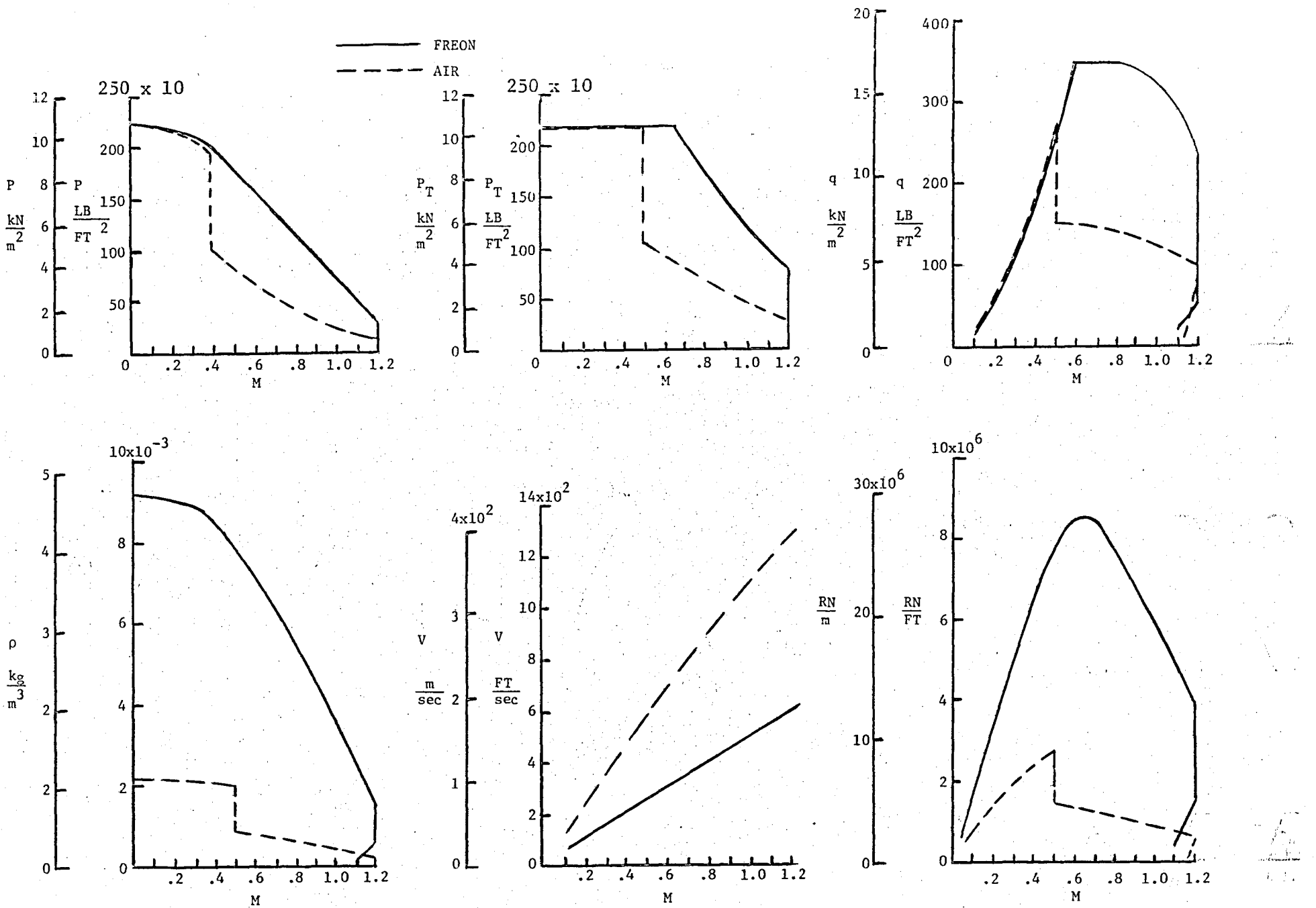

Figure 4.- Transonic Dynamics Tunnel operating boundaries $T_T = 130^0F$ (328^0K)

- TRANSONIC MACH NUMBER CAPABILITY - 0.1 TO 1.2
- TEST SECTION SIZE - 2.5m BY 2.5m (8.2 FT BY 8.2 FT)
- TEST MEDIUM - GASEOUS NITROGEN AND AIR
- CRYOGENIC TEMP. CAPABILITY - TEMPERATURE CONTROLLED INDEPENDENTLY FROM PRESSURE
  - ALLOWS SEPARATION OF STATIC AEROELASTIC (MODEL DEFORMATION) EFFECTS FROM RN (SCALE) EFFECTS SINCE DYNAMIC PRESSURE CAN BE VARIED WITH MACH NUMBER INDEPENDENTLY OF REYNOLDS NUMBER
  - SIX-FOLD INCREASE IN REYNOLDS NUMBER AT CONSTANT DYNAMIC PRESSURE
  - FOR EQUIVALENT MACH NUMBER, CRYO TEMP. CAPABILITY ALLOWS LOWER VELOCITY AND THEREFORE REDUCES SCALED FREQUENCY REQUIREMENTS
  - RELATIVELY LOW DRIVE POWER FOR RN CAPABILITY - 125,000 H.P.
- MODELS MOUNTED ON STING OR AT CONSTANT ANGLE OF ATTACK ON SIDEWALL
- CHANGE IN MACH NUMBER OF 0.1 IN 12-15 SEC.
- MODEL OBSERVED THROUGH TELEVISION MONITORS

Figure 5.- Characteristics of the National Transonic Facility

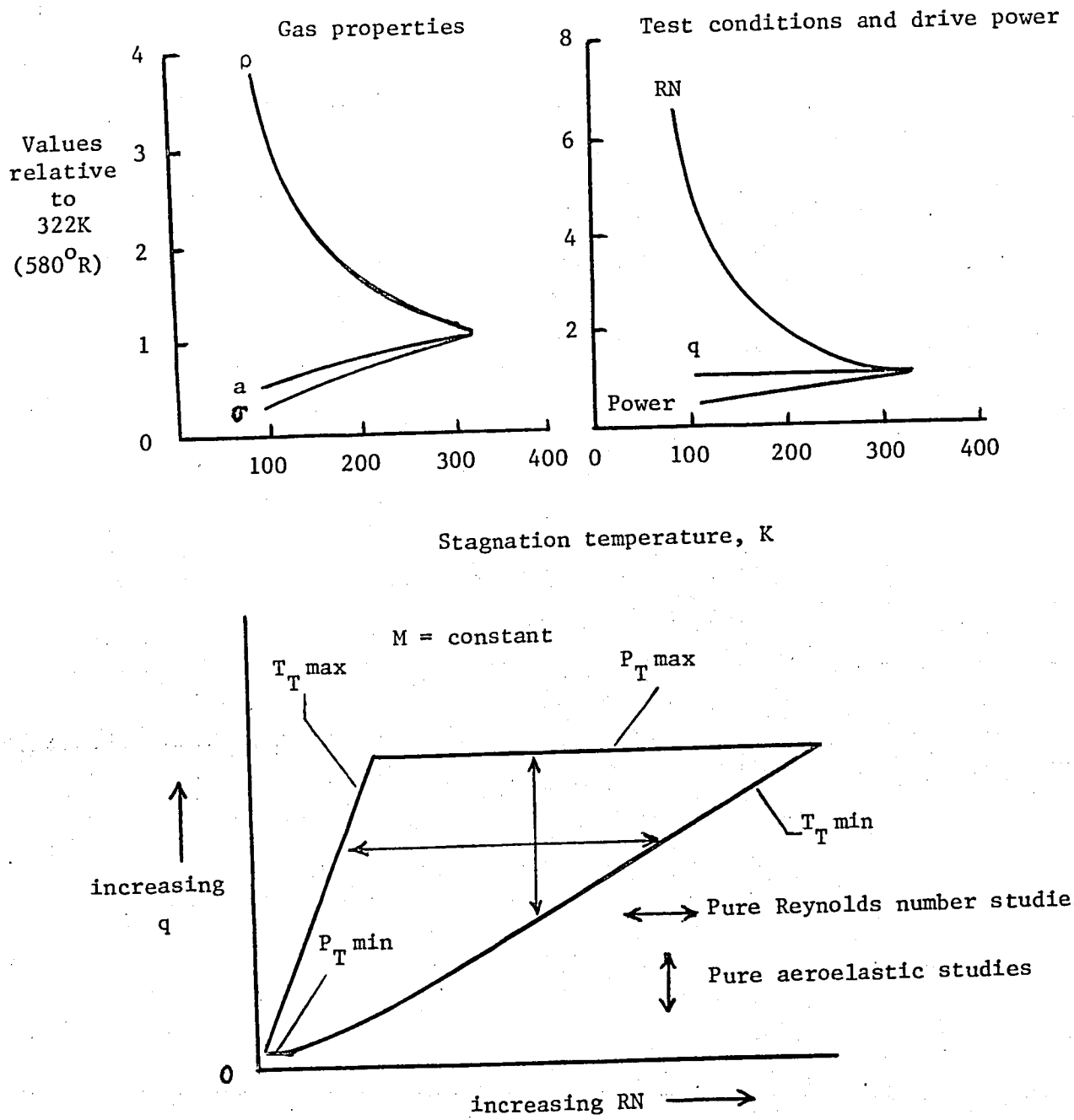

Figure 6.- Impact of having temperature as test variable in NTF.

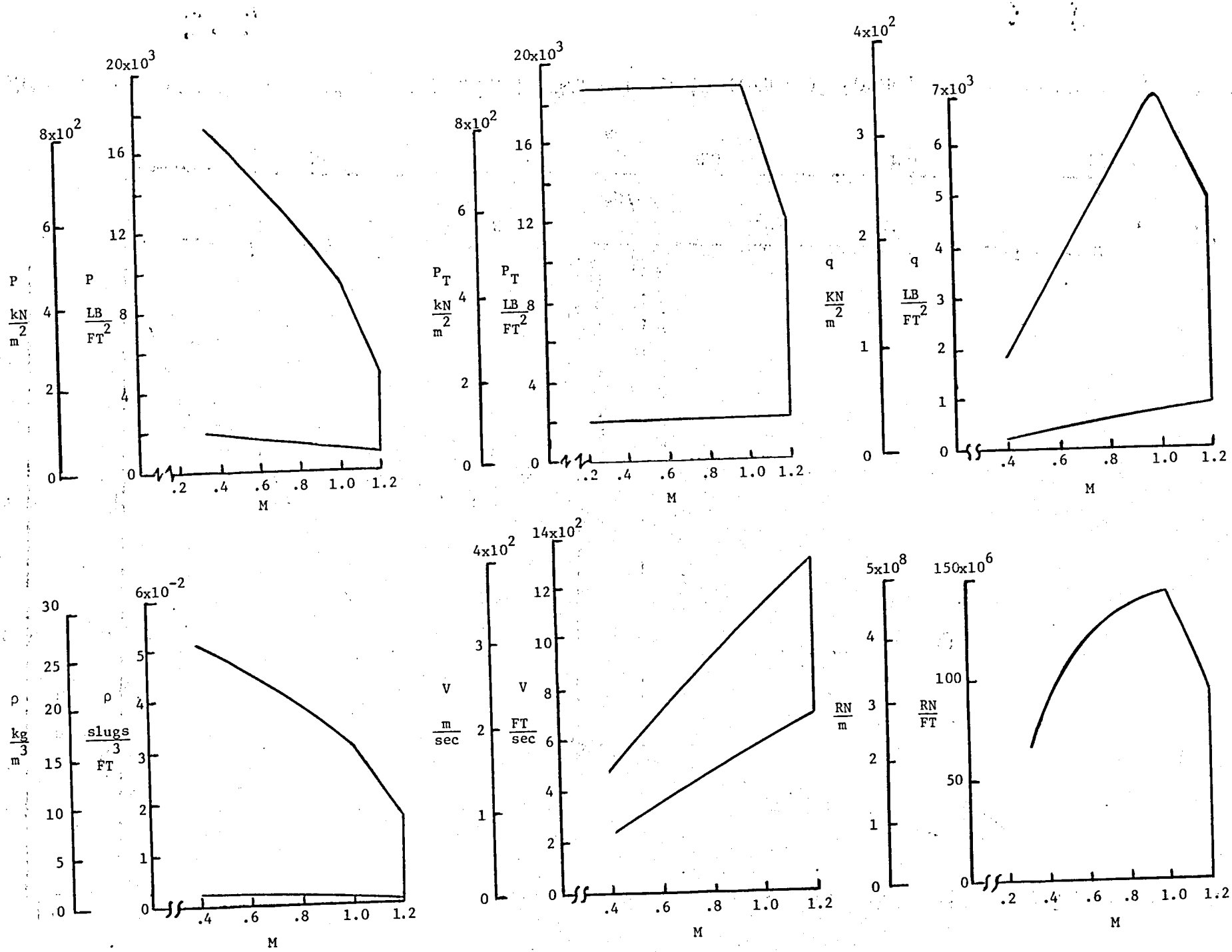

Figure 7.- NTF nominal maximum operating boundaries, T_T = -320°F to 175°F (78°K to 353°K).

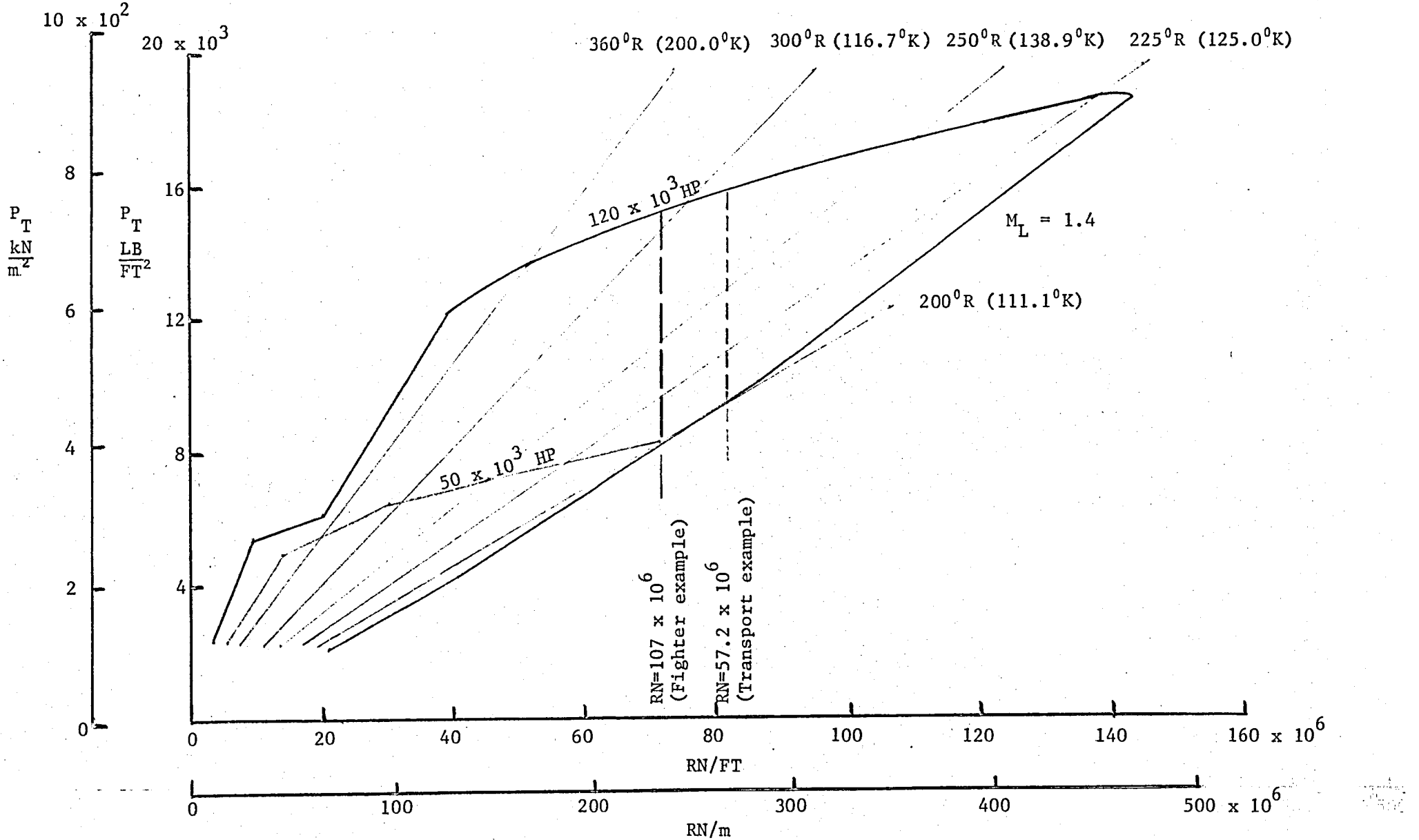

Figure 8.- NTF operating envelope replotted from ref. 3 in terms of Reynolds number per foot (meter)

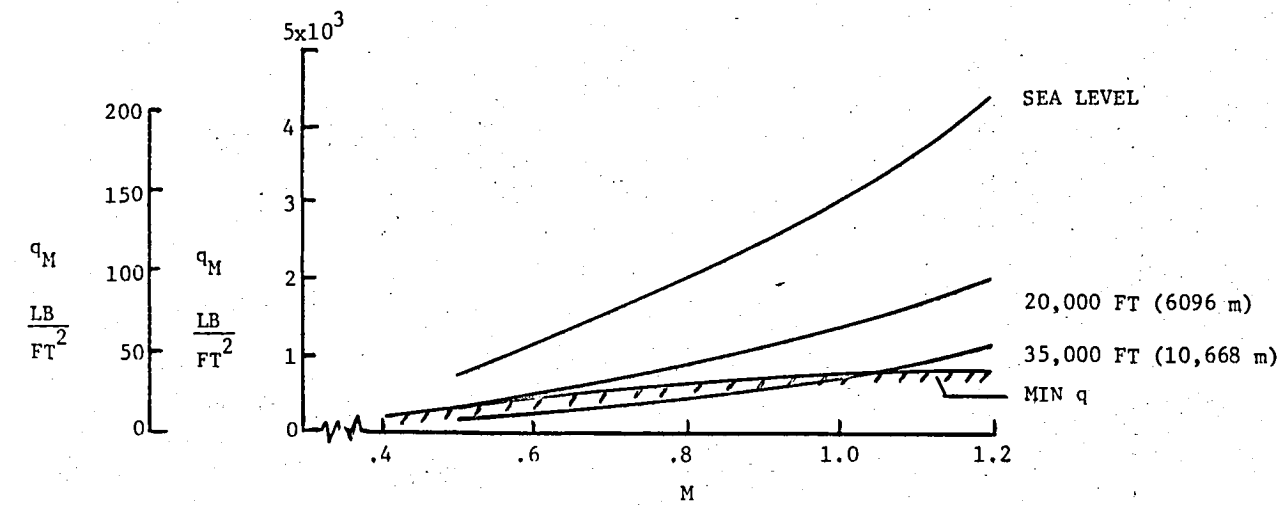

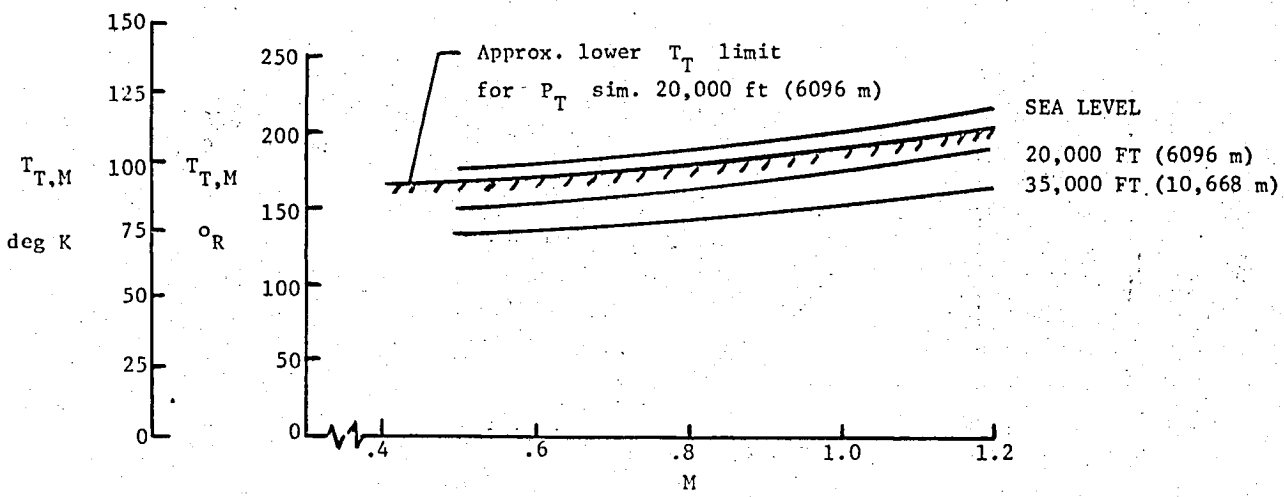

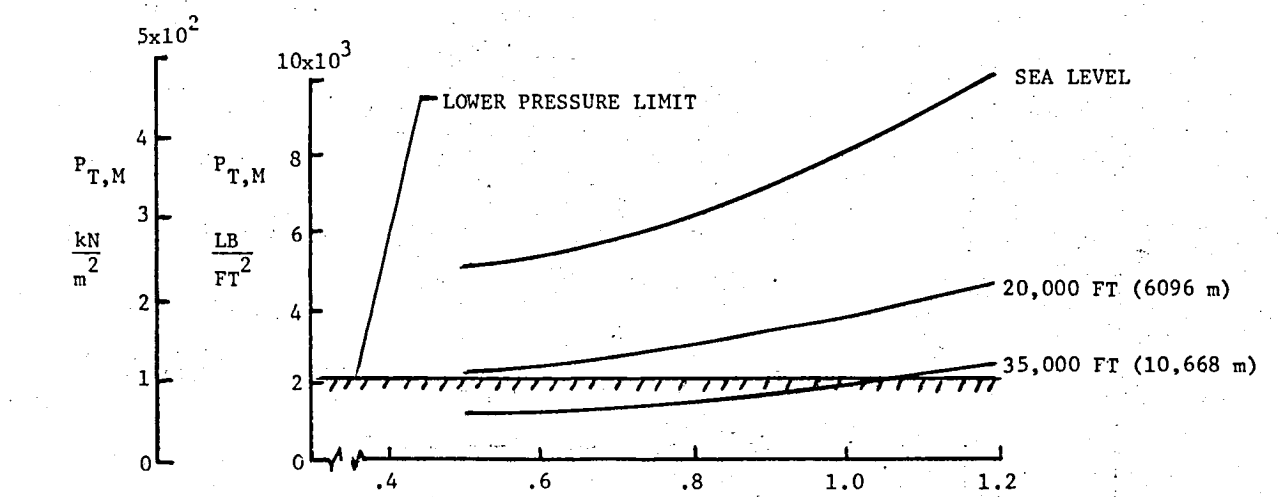

(a) Fighter Aircraft - Lowest pressure and temperature for full-scale RN

Figure 9.- Stagnation pressure and temperature and dynamic pressure required for model/airplane dynamic similarity.

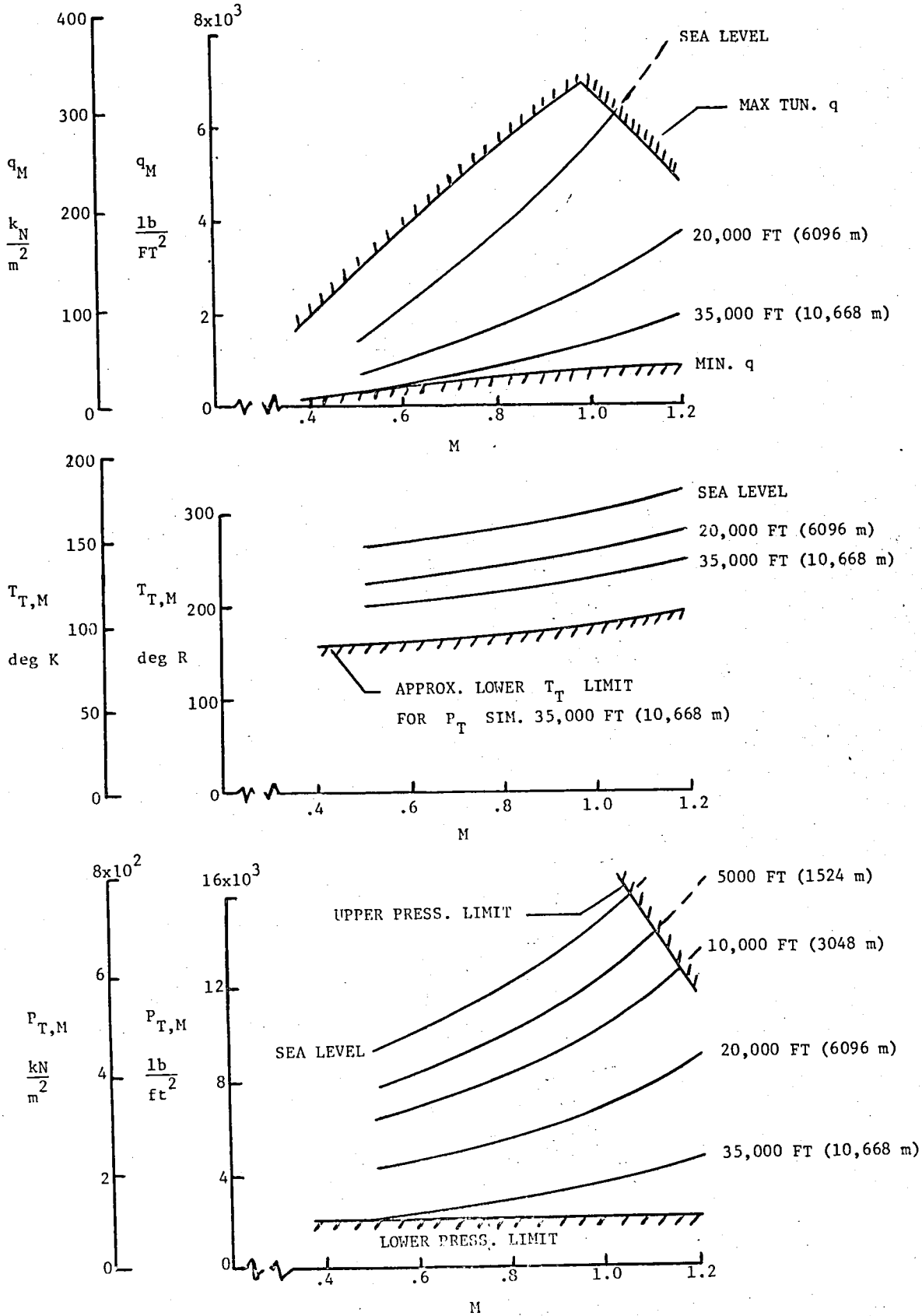

(b) Fighter Aircraft--Near-maximum pressure and temperature for full-scale RN

Figure 9.- Continued

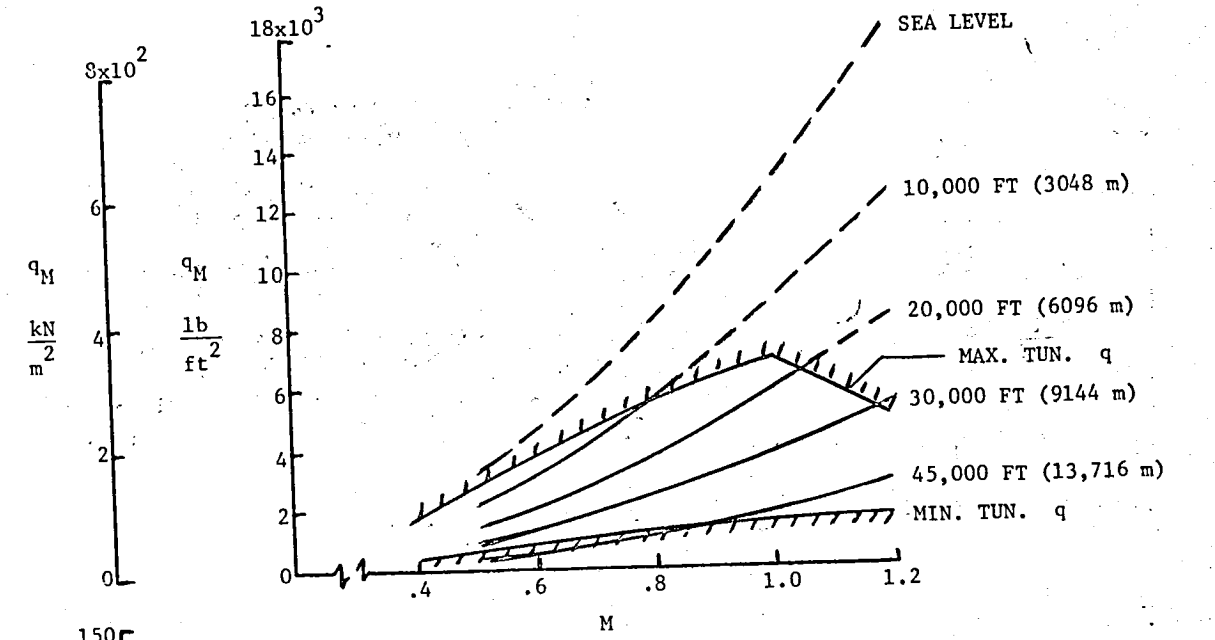

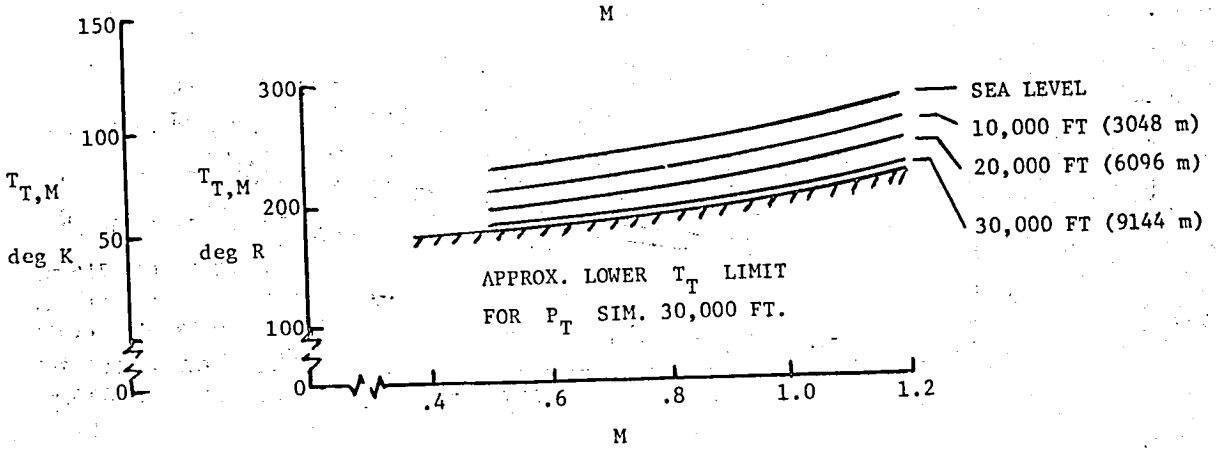

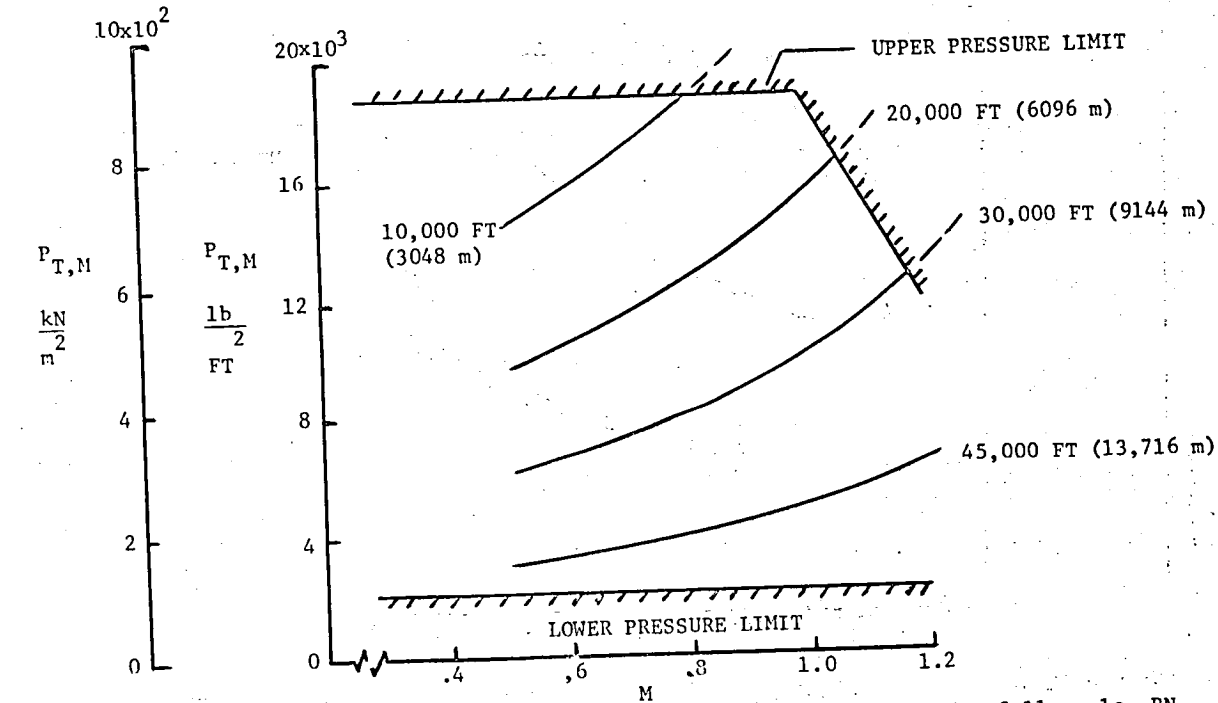

(c) Transport Aircraft--Lowest pressure and temperature for full-scale RN.

Figure 9.- Continued

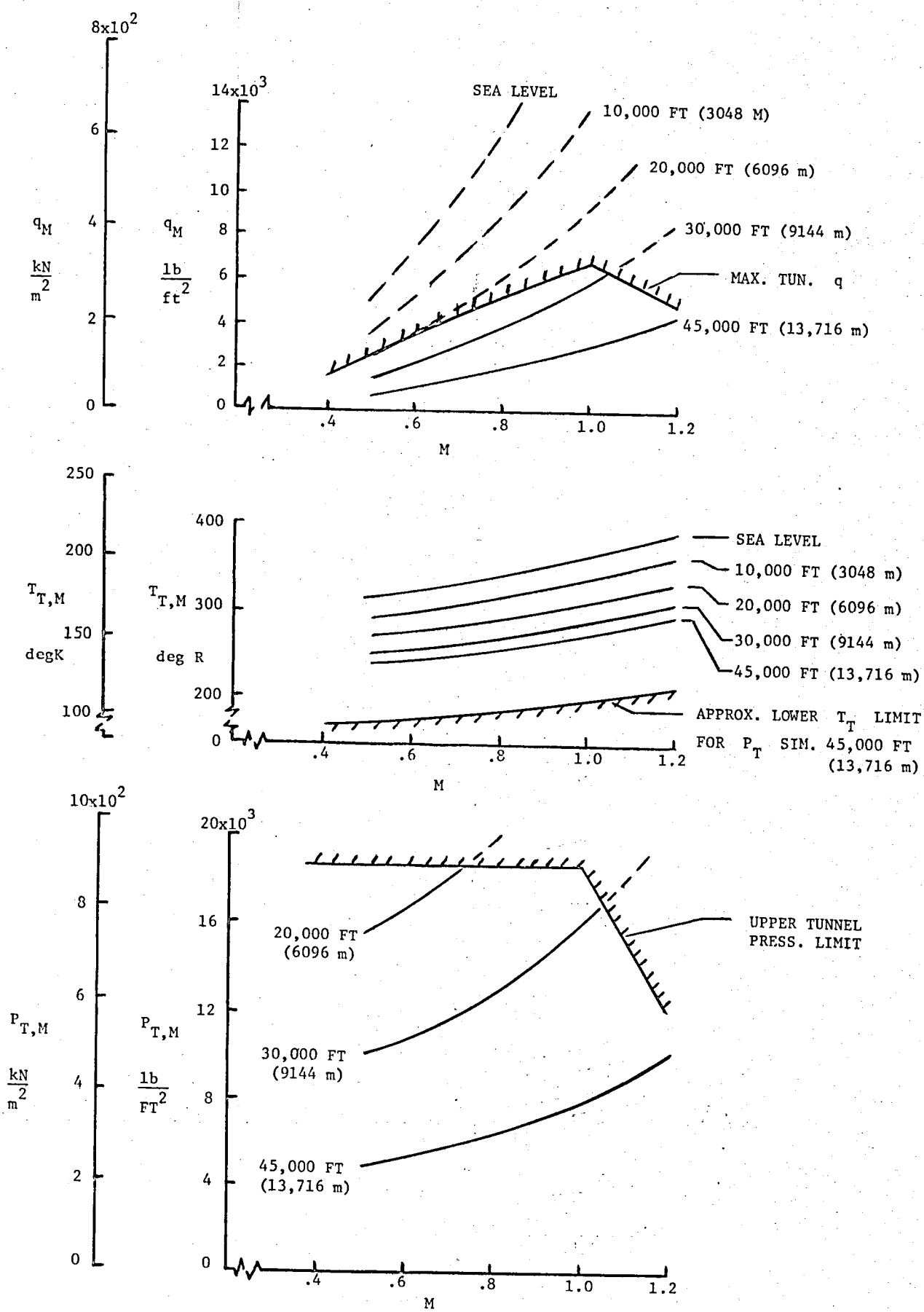

(d) Transport Aircraft--Near-Maximum pressure and temperature for full-scale RN.

Figure 9.- Concluded

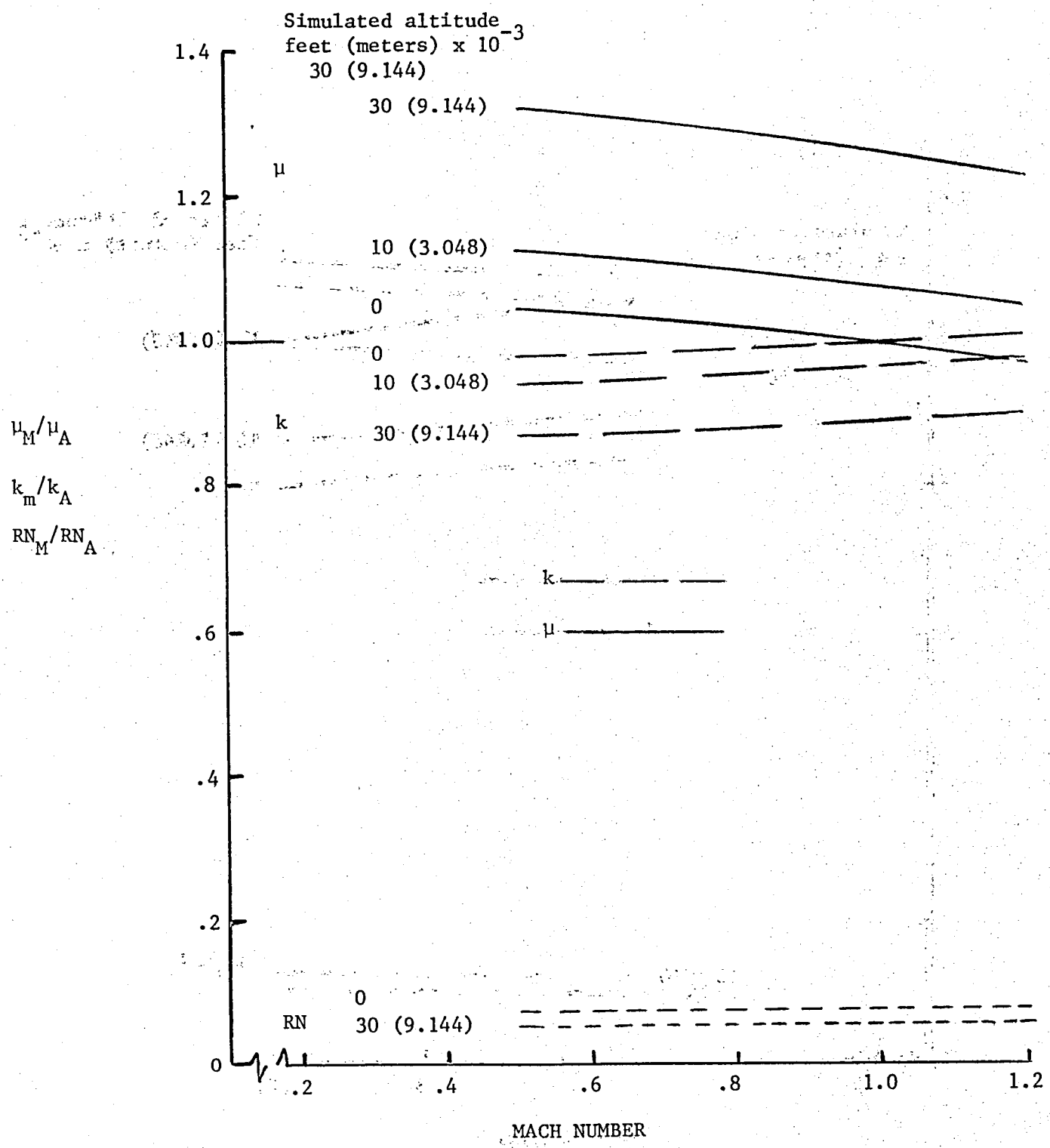

(a) Fighter airplane model.

Figure 10.- Variation of similarity parameters with Mach number and simulated altitude for testing in TDT. $T_{T,M}$ = 575°R (115°F).

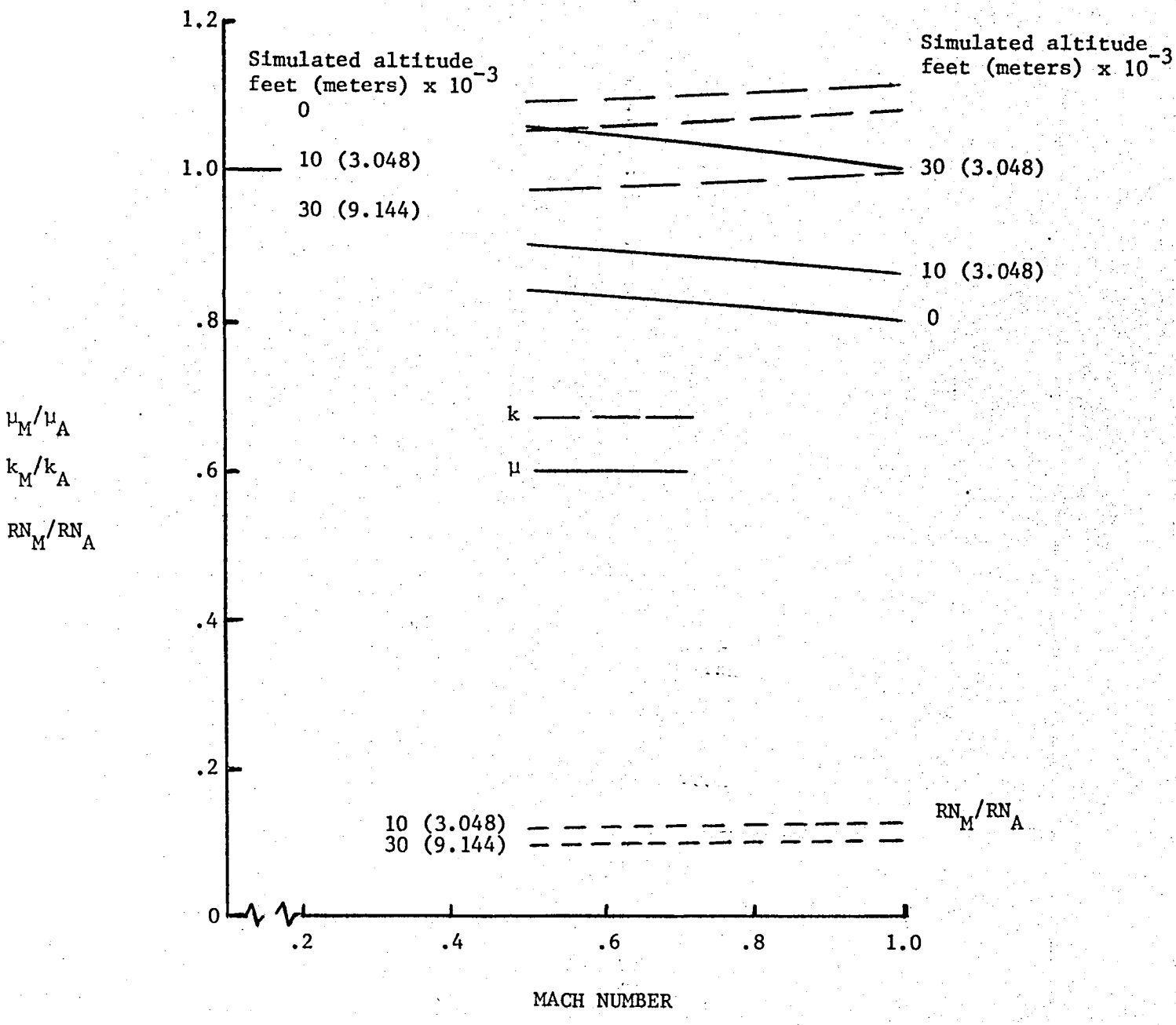

(b) Transport airplane model

Figure 10 .- Concluded.

PARAMETER	FIGHTER MODEL			TRANSPORT MODEL		
	NTF		TDT	NTF		TDT
	LOW TEMP.	HIGH TEMP.		LOW TEMP.	HIGH TEMP.	
b_M/b_A	0.1	0.1	0.2	0.035	0.035	0.07
span, ft	4.8	4.8	9.6	4.9	4.9	9.8
span (m)	1.46	1.46	2.93	1.49	1.49	2.99
b ft	1.5	1.5	3.0	0.7	0.7	1.4
b (m)	0.46	0.46	0.91	0.21	0.21	0.43
weight, lb	250	307	202	115	133	122
weight (kg)	113.4	139.3	91.6	52.2	60.3	55.3
ω_M/ω_A	5.67	6.94	2.27	18.51	21.78	7.26
m_M/m_A	5.27×10^{-2}	7.68×10^{-2}	5.04×10^{-2}	2.43×10^{-2}	2.43×10^{-2}	2.52×10^{-2}
$(EI)_M/(EI)_A$	2.013×10^{-4}	3.70×10^{-4}	2.08×10^{-4}	0.125×10^{-4}	0.20×10^{-4}	0.163×10^{-4}
μ_M/μ_A	1.0	1.0	0.98-1.32	1.0	1.0	0.89-1.06
k_M/k_A	1.0	1.0	0.87-1.01	1.0	1.0	0.97-1.06
F_M/F_A	3.21	4.82	1.01-1.36	12.0	16.6	6.49-7.46
RN_M/RN_A	1.0-1.09	1.0-1.05	0.06-0.08	0.97-1.02	0.97-1.00	0.10-0.12
TM ^oR	167-126	250-190	565-524	218-165	301-229	565-524
TM ^oK	92.8-70.0	138.9-105.6	313.9-291.1	121.1-91.7	167.2-127.2	313.9-291.1
q_M(max)psf	4300	6300	280	6300	6300	340
q_M(max), kN/sq m	205.9	301.6	13.4	301.6	301.6	16.3

Figure 11.- Summary of properties of example models scaled for the NTF and the TDT.

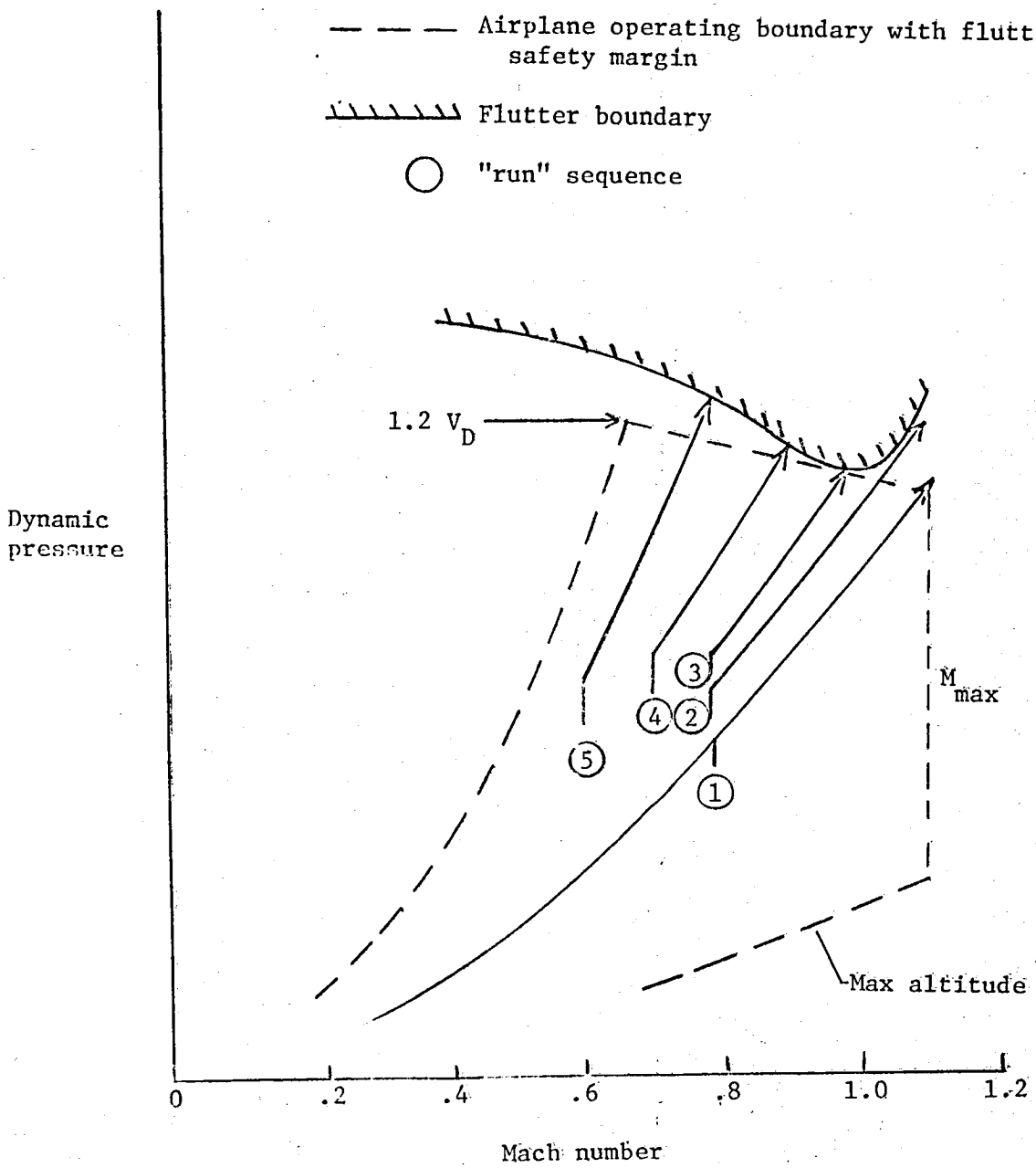

Figure 12.- Hypothetical flutter test used as a basis for cost comparisons for flutter testing in the NTF and the TDT.

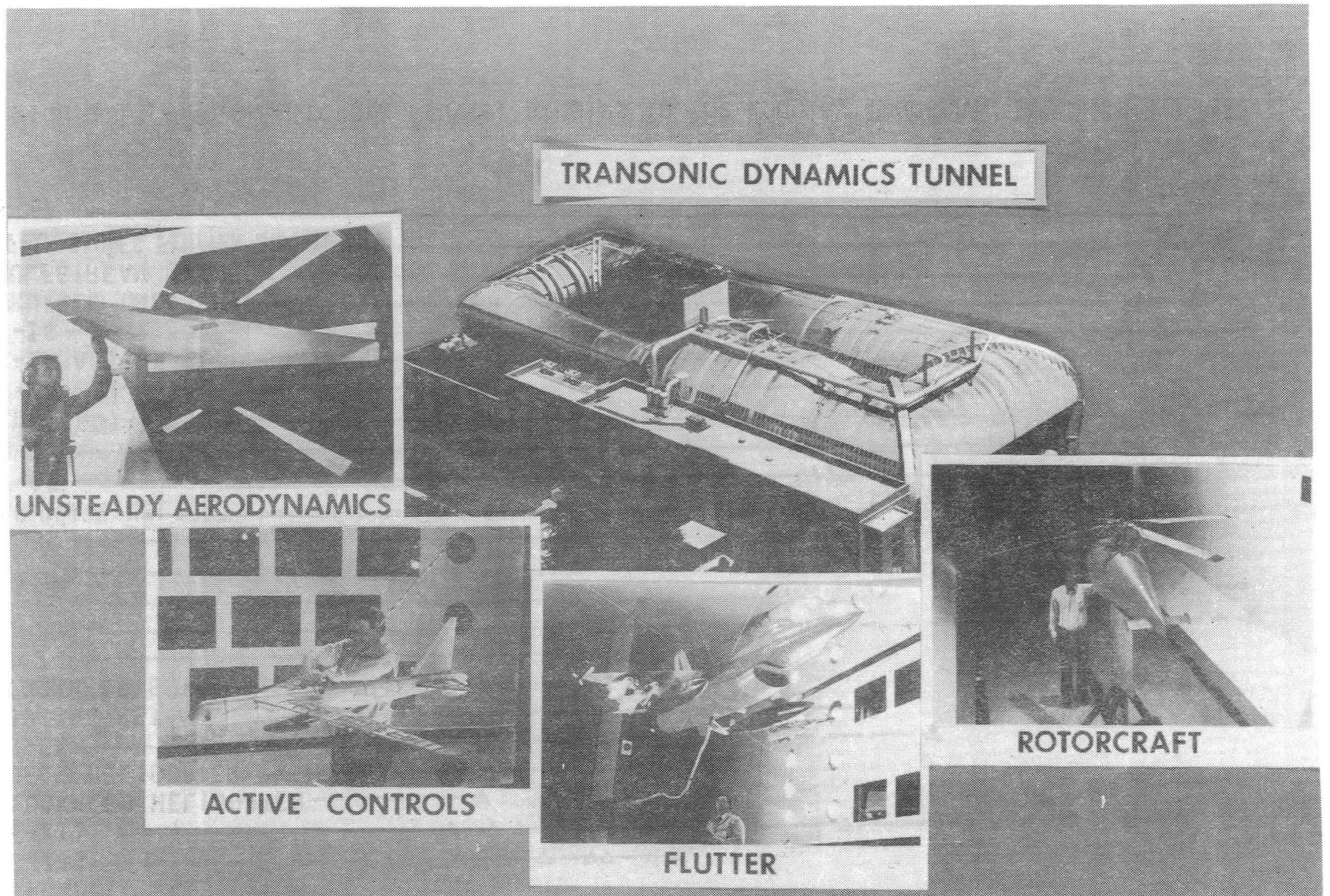

Figure 13.- Some technology areas supported by the Langley Transonic Dynamics Tunnel.

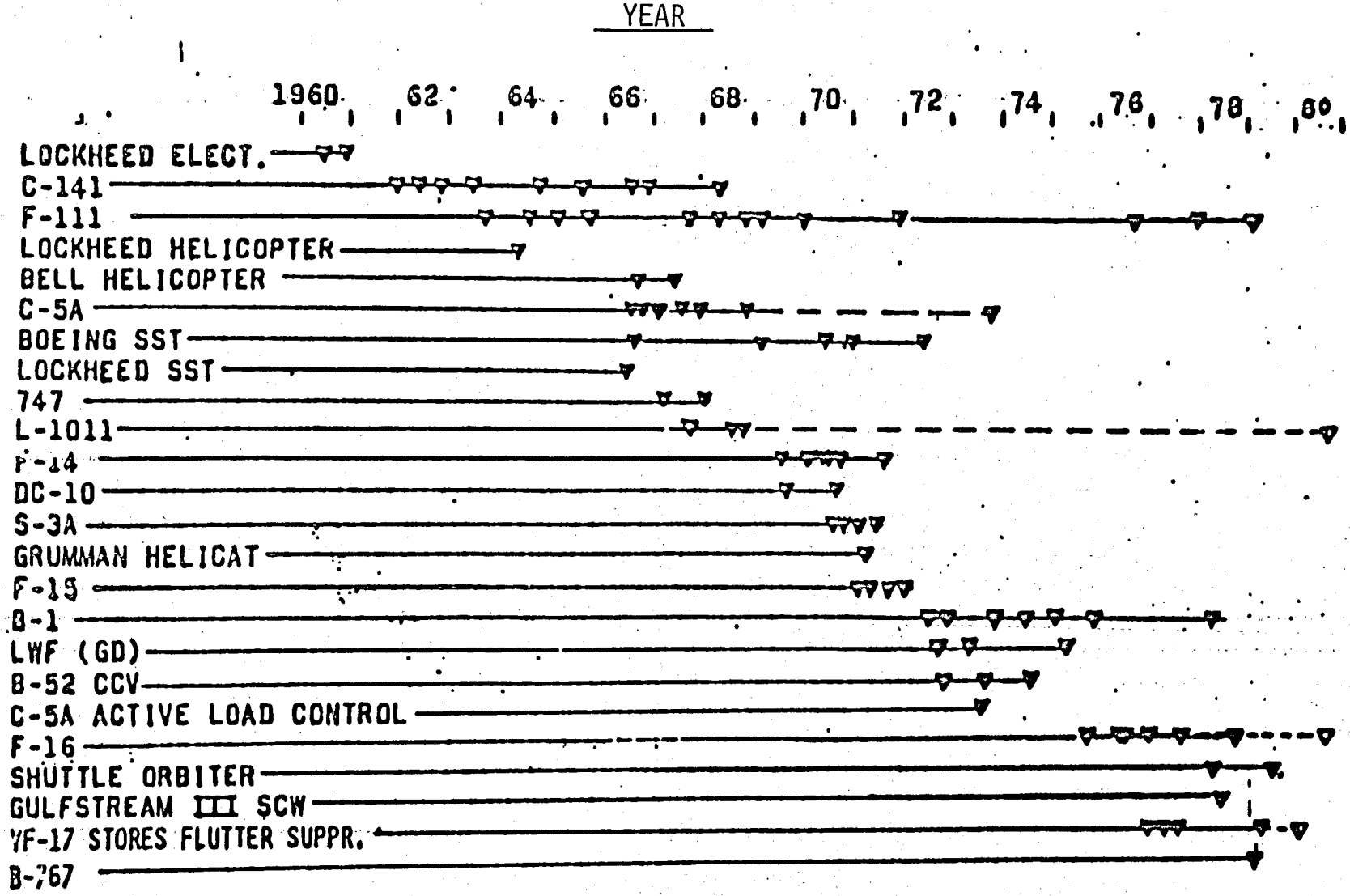

Figure 14.- Major aircraft flutter studies in the Langley Transonic Dynamics Tunnel.

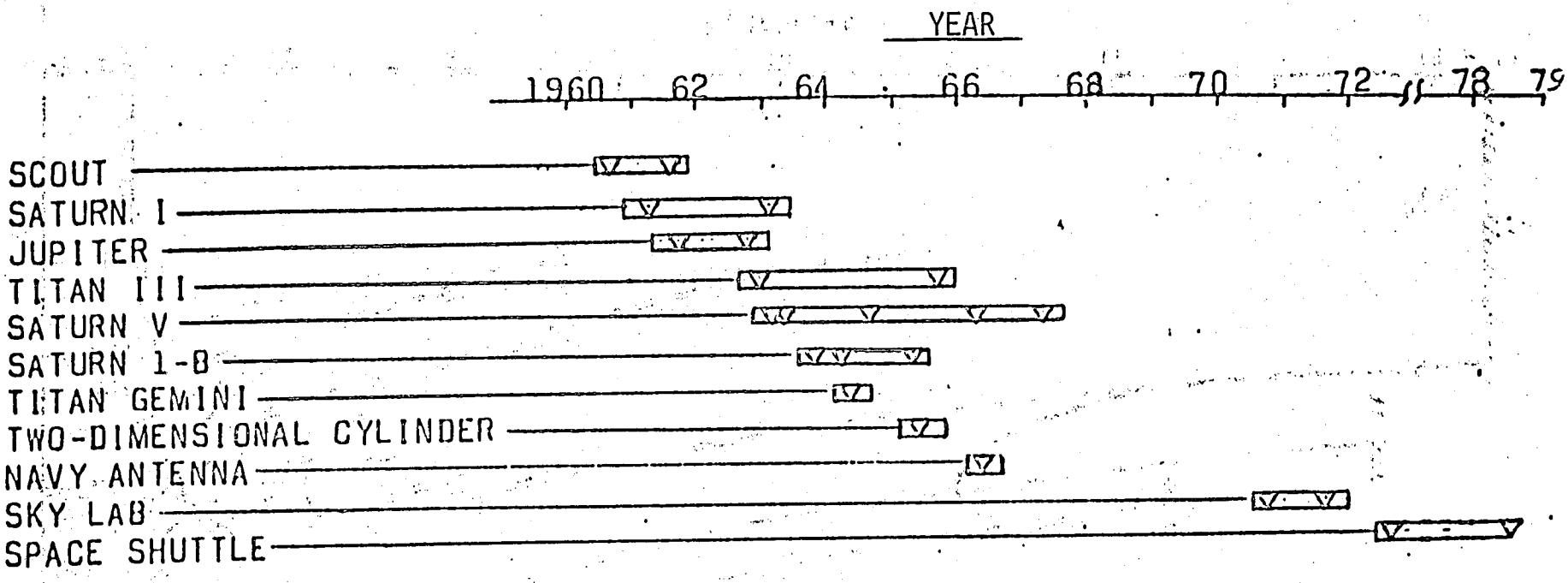

Figure 15. - Ground wind load studies in the Langley Transonic Dynamics Tunnel.

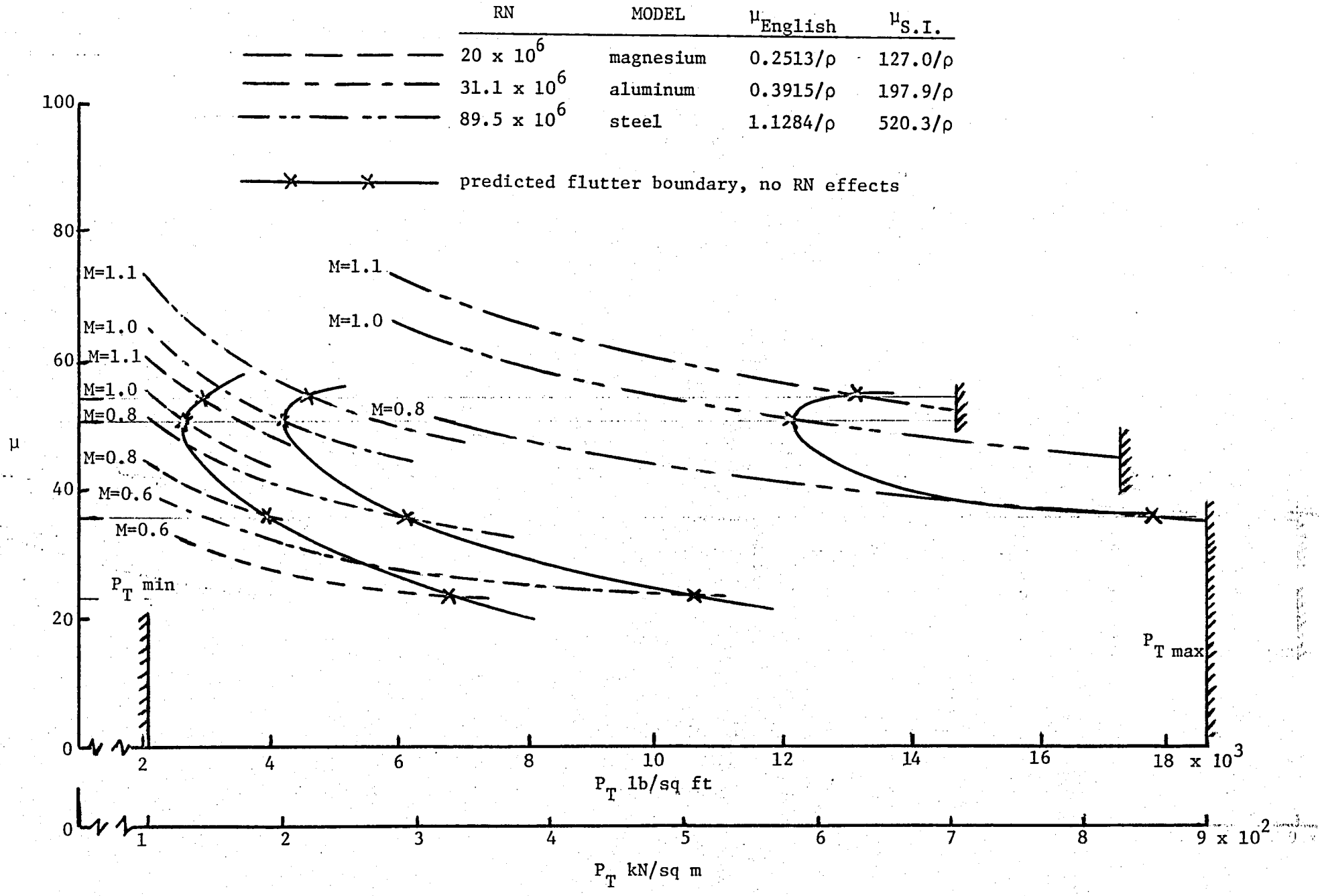

Figure 16.- Variation of mass density ratio of three models for three Reynolds numbers as a function of stagnation pressure at constant Mach number.

Mach No.	Mass-density ratio μ	Estimated tunnel conditions at flutter								
		Mag. model, RN = 20 x 10^6			Al. model, RN = 31 x 10^6			Steel Model, RN = 89.5 x 10^6		
		q, psf (kn/m^2)	P_T, psf (kn/m^2)	T_T °R (deg K)	q, psf (kn/m^2)	P_T, psf (kn/m^2)	T_T °R (deg K)	q, psf (kn/m^2)	P_T, psf (kn/m^2)	T_T °R (deg K)
0.6	23.2	1367 (65.5)	6873 (329.1)	310 (172.2)	2130 (102.0)	10,707 (512.7)	311 (172.8)	(1)	(1)	(1)
0.8	35.5	1172 (56.1)	3960 (189.6)	241 (133.9)	1826 (87.4)	6169 (295.4)	241 (133.9)	5263 (252.0)	17,782 (851.4)	241 (133.9)
1.0	50.5	1004 (48.1)	2697 (129.1)	200 (111.1)	1565 (74.9)	4202 (201.2)	200 (111.1)	5639 (270.0)	12,111 (579.9)	200 (111.1)
1.1	54.4	1179 (56.5)	2950 (141.3)	216 (120.0)	1825 (87.4)	4570 (218.8)	215 (119.4)	5263 (252.0)	13,173 (630.7)	215 (119.4)

Model physical characteristics: rectangular planform
semispan = 40 inches (1.016m)
chord length = 10 inches (0.254m)
bending freq. 15 Hz.
torsion freq. 57 Hz.
airfoil - 65A009
material - magnesium, aluminum, steel
weight - 14.7 lb. (6.67 kg) 22.9 lb. (10.39 kg) 66.0 lb. (29.94 kg)

(1) Estimated flutter q beyond tunnel power limit at M = 0.6

Figure 17.- Estimated tunnel conditions for simple flutter models in NTF.

1. Report No.	2. Government Accession No.	3. Recipient's Catalog No.
NASA TM-81839		

4. Title and Subtitle	5. Report Date
AN ASSESSMENT OF THE FUTURE ROLES OF THE NATIONAL TRANSONIC FACILITY AND THE LANGLEY TRANSONIC DYNAMICS TUNNEL IN AEROELASTIC AND UNSTEADY AERODYNAMIC TESTING	June 1980
	6. Performing Organization Code
7. Author(s)	8. Performing Organization Report No.
Perry W. Hanson	
	10. Work Unit No.
9. Performing Organization Name and Address	505-33-53-01
NASA Langley Research Center Hampton, VA 23665	11. Contract or Grant No.
	13. Type of Report and Period Covered
12. Sponsoring Agency Name and Address	Technical Memorandum
National Aeronautics and Space Administration Washington, DC 20546	14. Sponsoring Agency Code

15. Supplementary Notes

16. Abstract

The technological relationships between the National Transonic Facility (NTF) and the Langley Research Center Transonic Dynamics Tunnel (TDT), including the characteristics and capabilities of the two tunnels, that relate to studies in the fields of aeroelasticity and unsteady aerodynamics are discussed. Scaling considerations for aeroelasticity and unsteady aerodynamics testing in the two facilities are reviewed, and some of the special features (or lack thereof) of the TDT and the NTF that will weigh heavily in any decisions as to the relative merits of conducting a given study in the two tunnels are discussed. For illustrative purposes a fighter and a transport airplane are scaled for tests in the NTF and in the TDT, and the resulting model characteristics are compared. The NTF was designed specifically to meet the need for higher Reynolds number capability for flow simulation in aerodynamic performance testing of aircraft designs. However, it is concluded the NTF can be a valuable tool for evaluating the severity of Reynolds number effects in the areas of dynamic aeroelasticity and unsteady aerodynamics. On the other hand, the TDT was constructed specifically for studies and tests in the field of aeroelasticity. It is concluded that, except for tests requiring the Reynolds number capability of NTF, the TDT will remain the primary facility for tests in the areas of dynamic aeroelasticity and unsteady aerodynamics.

17. Key Words (Suggested by Author(s))	18. Distribution Statement
Flutter and buffet Wind tunnel capabilities Cryogenic temperatures Unsteady aerodynamics Dynamically scaled models	Unclassified - Unlimited Subject Category - 09

19. Security Classif. (of this report)	20. Security Classif. (of this page)	21. No. of Pages	22. Price*
Unclassified	Unclassified	50	A03

For sale by the National Technical Information Service, Springfield, Virginia 22161